



The expanding tropics: a critical assessment of the observational and modeling studies

Christopher Lucas,* Bertrand Timbal and Hanh Nguyen

This review provides comprehensive coverage of the tropical expansion literature to date. The primary focus is on the annual- and zonal-mean behavior of the phenomenon. An idealized model that identifies the mean meridional circulation as a hemisphere-wide structure with significant tropical–extratropical interaction is introduced as background for the understanding of the expansion and the methodologies used for detection. A variety of metrics from different data sources have been used to identify an expansion of the global tropics since 1979 by 1° – 3° latitude in each hemisphere, an average trend of approximately 0.5° – 1.0° decade⁻¹. The symmetry of this expansion—whether Northern and Southern hemispheres are expanding at the same rate—is unclear. Limitations of observational datasets, including reanalyses, prevent a more precise determination at this time. General circulation models are able to qualitatively reproduce this expansion, but generally underestimate its magnitude. Multiple factors have been identified as potential drivers of the expansion, including increasing greenhouse gases, stratospheric ozone depletion, and anthropogenic aerosols. No single factor by itself appears to explain the full expansion, perhaps a shortcoming of the models or experiment design. It may be that some combination of these forcings is producing the change, but the relative contribution of each forcing to the expansion is currently unknown. The key issues remaining to be resolved are briefly summarized at the end. © 2013 John Wiley & Sons, Ltd.

How to cite this article:

WIREs Clim Change 2013. doi: 10.1002/wcc.251

SUBTROPICAL DRYING AND TROPICAL EXPANSION

In recent decades, observations suggest that the hydroclimate in many regions has been changing. Reduced precipitation and more frequent droughts have been observed in southern portions of Australia,^{1,2} much of the Mediterranean region,^{3,4} portions of North America, particularly the southwestern United States,⁵ the Altiplano in South America,⁶ and northern China.⁷ Similar tendencies have also been noted in Africa and southeast Asia.^{8,9}

*Correspondence to: c.lucas@bom.gov.au

Centre for Australian Weather and Climate Research/Bureau of Meteorology, Melbourne, Vic, Australia

Conflict of interest: The authors have declared no conflicts of interest for this article.

While some places may only show seasonal rainfall declines, these deficits can drive extreme heat in later seasons.¹⁰ Droughts and precipitation have many natural influences across multiple timescales; teleconnections from changes in sea surface temperature (SST) driven by phenomena like the El Niño–Southern Oscillation (ENSO) or other decadal and centennial variability^{8,11,12} have a particularly noteworthy effect. However, some portion of the apparent trend may be linked to changes in the broader circulation patterns of the globe caused by anthropogenic global warming,⁸ trends that are projected to continue through the 21st century.⁹

A focus of these drying trends is found in the subtropics, among the driest regions on Earth. The subtropics are broadly associated with the downward branch of the Hadley circulation (HC), a planetary-scale tropical overturning circulation spanning half the

circulation. Only one hemisphere is shown; the full global MMC would be represented by a 'mirror image' in the other hemisphere. This view of the flow is developed from 'classical' meteorological concepts and studies using the (dry) isentropic streamfunction^{15,16} to diagnose the flow. Paluis et al.^{17,18} have developed a conceptually similar model based on a moist isentropic view of the circulation. These models differ from the more conventional 'three-cell' model based on the isobaric streamfunction, while still sharing many characteristics. The most notable differences are the enhanced extratropical circulation and the idea of a complex hemisphere-wide overturning circulation. This diagram and its discussion provide a qualitative framework for the methodologies and results discussed in this article.

In the tropics, many similarities to the three-cell model are observed. The flow is characterized by a deep meridional overturning circulation known as the Hadley circulation (HC). Mean ascent, driven by tropical mesoscale convective systems,¹⁹ is observed near the equator in the Intertropical Convergence Zone (ITCZ) with a broad compensating subsidence near 30° latitude. Radiative cooling drives much of the descent. In the lower-troposphere, the trade winds move air toward the equator; in the upper-troposphere, the flow moves poleward and terminates in the subtropical jet (STJ). Webster²⁰ provides a thorough elementary review of the characteristics and physics of the HC. The circulation varies with season and with the rising branch generally located off the equator by 5° latitude or more in the summer hemisphere. The descending branch also migrates with the season. The circulation in the winter hemisphere is significantly stronger than that in the summer hemisphere.²¹

Idealized axisymmetric models of the HC^{22,23} suggest that the HC width depends on the size and rotation rate of the Earth, the tropical tropopause height, and the pole-to-equator temperature gradient. In idealized aquaplanet simulations,²⁴ the width of the HC increases with increasing mean temperature and temperature gradient. Other experiments²⁵ indicate more complex relationships, with feedbacks between many different processes. No single parameter solely determines the scale of the HC. One important factor, often neglected in simpler models, is the effect of extratropical baroclinic eddies.²⁶ A significant role for these eddies has been suggested since the middle of the 20th century; Palmén and Newton²⁷ summarize this earlier work. Allowing for baroclinic instability suggests a dependence of the HC width on the gross static stability,²⁸ a relationship broadly supported in both idealized and realistic general circulation model

(GCM) simulations.^{24,29,30} This relationship has been found to apply in all seasons.³¹

In Figure 1, eddies dominate the circulation in the 'polar front', a symbiosis of the eddy-driven polar front jet (PFJ) and baroclinic waves. The polar front marks the position of the 'storm track', whose location and variability is related to the 'annular modes'.³² When the storm track is active, an overturning circulation similar to the Ferrel circulation is observed in association with the baroclinic waves and transient weather systems.³³ On average, the flow in the extratropics is quasi-isentropic. Moist air ascends in the polar front, resulting in enhanced precipitation, and returns equatorward, its moisture largely removed.³⁴ This circulation also varies seasonally, generally moving poleward and strengthening in the winter hemisphere, a response to greater baroclinicity. Significant longitudinal variability in wave activity arises from surface topographic features like mountain ranges and land-ocean boundaries.²⁷

The exact nature of the relationship between the extratropical eddies and the HC remains unclear and may also depend on season. Bordoni and Schneider³⁵ suggest that the impact of eddies on the HC is variable during the year. In their study of the Asian monsoon, they find that direct thermal driving becomes more important than eddies with the onset of the monsoon. Kang and Polvani³⁶ found a strong interannual relationship of the HC edge and the position of the eddy-driven jet in the Southern Hemisphere (SH) during summer, with the HC edge moving 1° latitude for a 2° shift in the position of the westerly jet. Ding et al.³⁷ show a linkage between tropical SST and the SH annular mode (SAM) through tropically forced Rossby wave trains.

In the idealized MMC model (Figure 1), tropical–extratropical interactions have the greatest impact in the subtropics, loosely defined as the region between the HC and the polar front. In general, the region is dominated by subsidence and the subtropical ridge (STR). In a relative sense, the air is dry and precipitation is low. Much of the variability here, on both seasonal and interannual time scales, is due to the continual evolution of tropical–extratropical interactions and their response to different forcings. For example, deep tropical convection—modulated by the Madden Julian Oscillation—has been shown to produce Rossby wave trains which extend well into the higher latitudes.³⁸

The stratosphere appears to play a significant role in the MMC. Much of its effect is related to ozone, and its observed depletion in recent decades.³⁹ The Antarctic ozone hole which forms every spring in particular has a significant impact on the MMC.

Increasing wind shear in the lower stratosphere has an effect on baroclinic waves, increasing their phase speed.⁴⁰ Stratospheric water vapor concentrations are known to affect the decadal rate of warming of the surface climate⁴¹ and these changing concentrations could drive changes in the tropospheric MMC.⁴² This is consistent with evidence that suggests that the stratospheric circulation changes precede anomalous tropospheric weather regimes. These stratospheric changes are translated to the troposphere through the annular modes.⁴³

The model represents the ‘typical’ structure of the MMC. At any given time or place, the represented features may be more or less prominent and/or in a different position. As noted earlier, seasonal variation is particularly important. Also, the seasonal evolution of the MMC is quite different in the two hemispheres; the variability of intensity and extent of the circulation is much larger in the Northern Hemisphere (NH) compared with the SH.²¹ The distribution of land, more prevalent in the NH, is an important factor in this different evolution.⁴⁴ Quasi-stationary waves, associated with mountain ranges, also play a role.⁴⁵ Rind and Perlwitz⁴⁶ suggest that topography is a factor in HC width based on a set of paleoclimate simulations. These factors also contribute to significant longitudinal variability in the behavior of the MMC, particularly in the extratropics.

OBSERVATIONS OF TROPICAL EXPANSION

A variety of datasets and/or metrics have been used in tropical expansion studies. From a practical standpoint, the definition of the ‘edge of the tropics’ is critical. With most metrics the point of transition from tropics to extratropics is neither intuitively obvious nor unambiguous, but rather is a transition occurring over a range of latitudes (i.e., the subtropics); defining ‘the edge’ is then a matter of choosing some point within this transition zone that is (hopefully) representative of the whole. The methods for making this choice can be subjective (but rationally decided) or objective (e.g., chosen through an algorithm), but ultimately the distinction is arbitrary. The subtleties of a complex region of the atmosphere are reduced to a single number that may or may not be representative of the behavior of the whole MMC. There is no universal definition of the tropical edge that is applicable across all datasets; each sees the transition zone in a different way and as such, the responses of a given metric show different sensitivities. Adding further complexity to these metrics are the effects of seasonal and/or longitudinal variability of the MMC; the zonal and

annual averaging used in many studies may introduce uncertainty or mask important processes in its own right. These aspects, along with the different time periods covered by different studies, confound the interpretation and comparison of the trends.

This section is organized around the different features of the MMC and/or datasets that have been used to identify the tropical edge. For each, a brief overview of the methodology is given and the results briefly discussed. A table is produced that summarizes the information from each study, including the data sources, the exact metric used, and the annual observed rate of expansion, given by hemisphere when available. As many studies here use the various global reanalysis products, references to those products and their acronyms are shown in Table 1.

Tropopause Methods

The tropopause height frequency (THF) methodology⁵⁵ is frequently used in tropical expansion studies. Outside of the subtropics, annual histograms of THF have a single peak. This peak is found at 15–17 km in the tropics and at 11–13 km in the extratropics. Within the subtropics, the THF is bimodal, an indicator used to define the tropical edge. The number of tropical tropopause days (TTD) is defined as the number of days that the tropopause exceeds a specified height threshold representative of the tropics. An array of TTD in time-latitude space is created and given values contoured. The slope of the contours provides an estimate of the long-term trend. Lu et al.⁵⁶ also applied this basic methodology.

The definition of the various thresholds is crucial. Generally, tropopause height thresholds from

TABLE 1 | Acronyms and References for the Reanalysis Products Discussed in the Article

Acronym	Expansion and References
NCEP	National Center for Environmental Prediction (NCEP)/National Center for Atmospheric Research (NCAR) Reanalysis ⁴⁷
ERA40	European Centre for Medium-Range Weather Forecasting (ECMWF) 40-year Reanalysis ⁴⁸
NCEP2	NCEP/Department of Energy (DOE) Reanalysis ⁴⁹
JRA25	Japanese 25-year Reanalysis ⁵⁰
ERA-I	ECMWF Interim Reanalysis ⁵¹
CFSR	NCEP Climate Forecast System Reanalysis ⁵²
20CR	NOAA-CIRES 20th Century Reanalysis ⁵³
MERRA	National Aeronautics and Space Administration (NASA) Modern Era Reanalysis for Research and Applications ⁵⁴

14.5 to ~16 km have been chosen, although there is some sensitivity to the choice of tropical tropopause threshold and the definition of the tropical edge.⁵⁷ This sensitivity arises, at least in part, from the observed global rise in tropopause heights⁵⁸ of ~40–80 m decade⁻¹,^{59–61} and the use of a fixed height threshold could act to confound the tropical expansion signal. Some studies^{57,58} define relative tropical tropopause thresholds to try and remove the effect of the ‘background’ tropopause trends. These methodologies reduce the magnitude of the tropical expansion trends. However, the amount of trend reduction has little apparent relationship with the time tendencies in the tropopause thresholds and the results are not robust.

A comparison of rates of THF-based tropical expansion in the SH computed directly from historical radiosonde data and from four reanalyses⁶² suggests that much of the sensitivity is related to issues with the underlying data quality; reanalysis-derived tropopause heights⁶³ are subject to strong biases in the subtropics. Global tropopause trends were estimated to have a small effect on the estimated expansion trends (less than 0.1° decade⁻¹).⁶²

A blended tropopause height dataset⁶¹ derived from the two ECMWF reanalyses combines thermal and dynamic definitions of the tropopause is also used to examine expansion rates. This dataset reduces the bias in the subtropics. The THF methodology is not used in this study, but expansion rates are consistent with those studies. A non-THF tropopause-based methodology—the potential temperature difference between the tropopause and the surface ($\Delta\theta$), a dry bulk stability parameter—has also been used to identify the edges of the tropics and its long-term trend.⁶⁴

Table 2 summarizes the results from studies using a tropopause-based metric. For the most part, these indicate an expansion of less than 1° decade⁻¹ in each hemisphere. Many THF-based studies indicate that the SH has expanded more rapidly than the NH. Results with relative thresholds^{57,58} generally show smaller trends and even contraction in some cases. The results are dependent on the reanalysis chosen. In several studies, significant interannual variability is identified,^{56,58,62} with effects due to ENSO and large volcanic eruptions noted. Seasonal differences in tropopause-based trends may also be present, generally suggesting a weak tendency toward greater

TABLE 2 | Summary of Studies Using the Tropopause-Based Methodologies

Investigators	Data Sources	Thresholds	Time Period	Expansion (° Latitude Decade ⁻¹)
Siedel and Randel ⁵⁵	NCEP, ERA40 radiosondes	15.5 km/TTD = 300, 200, or 100	1979–2005	Both: 1.7–3.1 Equal between hemispheres
Lu et al. ⁵⁶	NCEP and ERA40	120 hPa/200 days	1958–1999	SH: 0.5–0.7 NH: 0.05–0.2
Birner ⁵⁷	NCEP, NCEP2, ERA40, and JRA25	Variable/equivalent latitude	1979–2008	SH: –0.4 to 0.7 NH: –0.2 to 0.0
	NCEP, NCEP2, ERA40, and JRA25	Variable 2/equivalent latitude	1979–2008	SH: 0.0–0.6 NH: –0.2 to 0.2
Wilcox et al. ⁶¹	S ERA-I, ERA40 blended tropopause	Average of 15.0, 15.5, and 16.0 km/NA	ERA40: 1958–2001 ERA-I: 1989–2007	ERA40 Both: 0.7 ERA-I Both: 0.9 (60–80% in SH)
Davis and Rosenlof ⁵⁸	S NCEP, CFSR, JRA25, and MERRA	15.0 km/equivalent latitude	1979–2009	SH: 0.2–0.8 NH: –0.1 to 0.6
	S NCEP, CFSR, JRA25, and MERRA	Variable, 1.5 km below tropical mean/equivalent latitude	1979–2009	SH: 0.1–0.4 NH: –0.3 to 0.3
Lucas et al. ⁶²	Radiosonde	14.5 km/200 days	1979–2010	SH: 0.4, regionally varies 0.2–0.6
Davis and Birner ⁶⁴	MERRA, ERA-I, and NCEP	Subtropical stability maxima	1979–2010	Both: –0.5 to 0.9

Positive values equal expansion regardless of hemisphere. Thresholds refer to tropical tropopause height threshold and the number of TTD used to define the edge. An ‘s’ after the investigators indicates the study examined the seasonality of the expansion. NH, Northern Hemisphere; SH, Southern Hemisphere.

expansion in the summer and autumn months of each hemisphere^{58,61} although these trends are not always statistically significant.⁵⁸ Longitudinal variability in the amount of tropical expansion was also noted with this methodology.⁶²

Satellite Methods

Varied metrics derived from satellite-based platforms have been widely used to investigate tropical expansion. One common method is analogous to the THF methodology; zonal averages of the metric are arranged in a time-latitude array, a definition of the tropical edge chosen, and trends estimated from the slope of chosen contours. As with the THF methodology, background trends in the quantity of interest may mask the true rate of tropical expansion.

A common metric in satellite studies is outgoing longwave radiation (OLR).^{58,65,66} Since 1979, broad trends have been noted in many OLR datasets, on the order of 1–3 W m⁻² decade⁻¹, depending on the dataset and the area examined.^{58,67–69} Several recent studies^{70,71} have examined cloudiness measurements

from the International Satellite Cloud Climatology Project (ISCCP)⁷² and the Pathfinder Atmosphere (PATMOS)⁷³ datasets, defining the position of the edge from either a fixed threshold or the minimum in subtropical cloudiness. One study⁷⁴ examined the long-term changes in different NH ozone regimes derived from satellite data, whose boundaries are closely linked with upper-tropospheric fronts.⁷⁵ A later study⁷⁶ used this approach to extend these results into the SH. Trends in upper-troposphere and lower-stratosphere temperature data retrieved from the (Advanced) Microwave Sounding Unit (MSU/AMSU) have also been used to infer tropical expansion, either through analysis of global temperature trends⁷⁷ or changes to the idealized temperature structure associated with the STJ.⁷⁸

Table 3 summarizes the satellite-based studies. Large differences exist in many estimates using the same or similar data sources. Four OLR datasets each shows a general widening trend in both hemispheres, greater in the NH.^{65,66} However, differences between the datasets are large, in some cases statistically significant.⁵⁸ Using a relative threshold reduces the

TABLE 3 | Summary of Studies of Tropical Expansion Using Satellite-Based Methodologies

Investigators	Data Sources	Metric	Time Period	Expansion (° Latitude Decade ⁻¹)
Hudson et al. ⁷⁵	Satellite-derived ozone	Total ozone	1979–2003 1979–1991	NH: about 1° NH: 1.1
Fu et al. ⁷⁷	MSU	Global temperature trends	1979–2005	Estimated total shift of 1° per hemisphere
Hu and Fu ⁶⁵	S HIRS, ISSCP, and GEWEX	Monthly OLR, 250 W m ⁻²	1984–2004 1980–2003 (HIRS)	SH: 0.3–0.9 NH: 0.6–1.1
Johanson and Fu ⁷⁹	HIRS, ISSCP, and GEWEX	Multidataset OLR, 250 W m ⁻²	1984–2004 1979–2003 (HIRS)	Both: 3.0
Hu et al. ⁶⁶	S NOAA	OLR, 250 W m ⁻²	1979–2009	SH: 0.3 NH: 0.9
Fu and Lin ⁷⁸	3 MSU datasets	Lower stratospheric temperature	1979–2009	SH: 0.2 NH: 0.3
Zhou et al. ⁷⁰	S ISSCP cloudiness	Subtropical 60% coverage	1984–2006	SH: 0.7–1.3 NH: 1.3–1.6
	S ICCSP cloudiness	Subtropical cloud cover minimum	1984–2006	SH: -0.1 to -0.6 NH: 0.3–1.6
Davis and Rosenlof ⁵⁸	S NOAA, HIRS, GEWEX, and ISSCP	OLR/variable: 20 W m ⁻² below subtropical maximum	1979–2005, 1979–2009 for NOAA	SH: -0.3 to 0.4 NH: 0.1–0.5
Allen et al. ⁷¹	ISSCP, AVHRR cloud climatology	Subtropical cloud cover minimum	1983–2008	SH: 0.36 NH: 0.39
Hudson ⁷⁶	Satellite-derived ozone	Total ozone	1979–2010	SH: 2.0 NH: 1.2

Positive values equal expansion regardless of hemisphere. An 'S' after the investigators indicates the study examined the seasonality of the expansion. NH, Northern Hemisphere; SH, Southern Hemisphere.

magnitude of the trends, such that two OLR datasets suggest contracting trends in the SH.⁵⁸ The studies using minimum cloudiness metrics show considerably different results,^{70,71} with differing signs in the SH. Global temperature trends suggested a total shift in the jet stream of about 1° in each hemisphere,⁷⁷ later refined to identify total expansions of 1° in the NH and 0.6° in the SH.⁷⁸ Studies using ozone data^{74,76} indicate a broadening of about 1° decade⁻¹ in the NH, particularly between 1979 and 1991. In the SH, expansion using this methodology has averaged 2.0° decade⁻¹ between 1979 and 2010. The OLR-based studies show only weak signals of seasonal variability.^{58,65,66} Inter-annual variability was not discussed.

Streamfunction Methods

One common metric is the edge of the HC as derived from calculations of the (isobaric) mass streamfunction (Ψ).^{21,58,64,65,71,79,80} The mass streamfunction is a vertical integral of the meridional wind and produces the familiar three-cell model of the MMC. The edge of the tropics is generally taken as the latitude of the subtropical zero isopleth in the mid-troposphere. The monthly position of the HC is determined, which can be averaged to the desired resolution and tracked in time to estimate the expansion. This metric, annually averaged, for eight reanalysis products is shown in Figure 2. Visual examination of the time

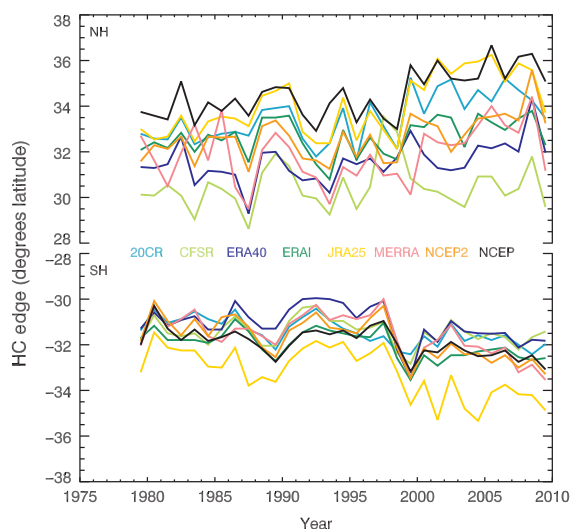


FIGURE 2 | Time series of the position of the subtropical edge of the Hadley cell as defined from the streamfunction in the eight modern reanalyses for the Northern (top) and Southern (bottom) Hemisphere. (Reprinted with permission from Ref 21. Copyright 2013 The American Meteorological Society). Time series from ERA40 (post 2002) and 20CR (post 2008) are partially extrapolated from statistical relations with the other reanalyses.

series shows an expansionary trend is apparent in each hemisphere—particularly the NH—although considerable scatter exists in the estimates.

Table 4 summarizes the Ψ -based results. Overall, expansion rates are below 0.8° decade⁻¹, with little difference between the hemispheres.^{21,58,65} Studies that examine both hemispheres combined^{64,79,80} suggest expansion rates of 0.4 and 3.2° decade⁻¹. No studies using this methodology indicate contraction. Seasonally, expansion is more rapid in the respective summer and autumn seasons of each hemisphere,^{21,58,65} when the HC is extended furthest poleward and its intensity is lowest. Despite the large trends, the NH expansion in many reanalyses is not statistically significant due to high variability within the time series.²¹ The SH expansion is more robust across the different products, with a shift in the location indicated across all reanalyses in the late 1990s (Figure 2).

Jet Stream Methods

Another metric used to examine tropical expansion is the change in position of the various jet streams, which can be defined in different ways. Several studies^{58,81} identify jet streams in several reanalyses from the mass-weighted wind between 400 and 100 hPa. Jet streams have also been defined from the zonal-mean zonal wind at 850 hPa and from the location of the speed maxima of the jet streams as defined above.^{58,64} The NH 850 to 300 hPa maximum wind derived from radiosonde data has also been investigated.⁷¹ While not explicitly considered in this section, the satellite temperature study noted earlier interpret their data based on an idealized model of the STJ, although no wind data are actually used there.⁷⁸

Table 5 shows the trends based on these metrics. For the jet streams defined from the mean wind, trends of less than 0.2° decade⁻¹ are generally observed. No consistent difference is noted between upper and lower jet streams in these metrics.^{58,81} When using the latitude of the maximum mean wind, the time series are much more variable and hence have greater uncertainty in the trend values.⁵⁸ This is particularly notable for the 850 hPa zonal winds in the SH, where some individual reanalyses identify contractive trends on an annual basis.⁵⁸ The seasonality of the trends is inconsistent across the metrics. For zonal-mean wind metrics, the seasonality tends to be weaker. For those based on maxima, the seasonality is larger with changes of sign and strength throughout the year. For the 850 hPa maximum wind defined edge in the SH, expansion is noted in summer and autumn while strong contraction is noted in winter and spring.⁵⁸

TABLE 4 | Summary of Studies Using Streamfunction (Ψ) Methods

Investigators	Data Sources	Metric	Time Period	Expansion (°Latitude Decade ⁻¹)
Hu and Fu ⁶⁵	S NCEP, ERA40, and NCEP2	Isobaric mass streamfunction	1979–2005	SH: 0.4–1.2 NH: 1.0–2.3
Johanson and Fu ⁷⁹	NCEP, ERA40, and NCEP2	Multidataset average isobaric mass streamfunction	1979–2004	Both: 3.2
Stachnik and Schumacher ⁸⁰	S NCEP, ERA40, NCEP2, ERA-I, MERRA, CFSR, JRA25, and 20CR	Isobaric mass streamfunction	1979–2008	Both: 1.10 (ensemble) Range: 0.29–1.48
Davis and Rosenlof ⁵⁸	S NCEP, JRA25, CFSR, and MERRA	Isobaric mass streamfunction	1979–2009	SH: 0.1–0.8 NH: 0.1–0.8
Allen et al. ⁷¹	NCEP, NCEP2, ERA40, MERRA, and CFSR	Multidataset average isobaric mass streamfunction	1979–1999	SH: 0.36 ± 0.3 NH: 0.42 ± 0.2
Nguyen et al. ²¹	S NCEP, ERA40, NCEP2, ERA-I, MERRA, CFSR, JRA25, and 20CR	Isobaric mass streamfunction	1979–2009	SH: 0.1–0.8 NH: 0.2–1.0
Davis and Birner ⁶⁴	MERRA, ERA-I, and NCEP	Isobaric mass streamfunction	1979–2010	Both: 0.4–2.0

Positive values equal expansion regardless of hemisphere. An ‘S’ after the investigators indicates the study examined the seasonality of the expansion. NH, Northern Hemisphere; SH, Southern Hemisphere.

TABLE 5 | Summary of Studies Using Jet Stream Methods

Investigators	Data Sources	Metric	Time Period	Expansion (°Latitude Decade ⁻¹)
Archer and Caldeira ⁸¹	NCEP and ERA40	Mean latitude of mean 400 to 100 hPa wind	1979–2001	SH: 0.06–0.12 NH: 0.17–0.19
Davis and Rosenlof ⁵⁸	S NCEP, JRA25, CFSR, and MERRA	Mean latitude of mean 400 to 100 hPa wind	1979–2009	SH: 0.0–0.1 NH: 0.0–0.1
	S	Mean latitude of mean 850 hPa wind	1979–2009	SH: 0.0–0.2 NH: 0.1–0.3
	S	Latitude of maximum 400 to 100 hPa wind	1979–2009	SH: 0.1–0.3 NH: 0.0–0.2
	S	Latitude of maximum 850 hPa wind	1979–2009	SH: –0.4 to 0.2 NH: 0.0–0.2
Allen et al. ⁷¹	Radiosonde	Latitude of 850 to 300 hPa wind	1979–2009	SH: 0.20 NH: 0.08
Davis and Birner ⁶⁴	MERRA, ERA-I, and NCEP	Latitude of maximum wind	1979–2010	Both: 0.3–0.6

Positive values equal expansion regardless of hemisphere. An ‘S’ after the investigators indicates the study examined the seasonality of the expansion. NH, Northern Hemisphere; SH, Southern Hemisphere.

Surface-Based Methods

Several studies rely upon surface-based variables to investigate tropical expansion. Several studies^{66,70,71} utilize the Global Precipitation Climatology Project (GPCP) monthly dataset^{82,83} to examine shifts in the locations/boundaries of the subtropical dry zones, as defined by the location of the precipitation minimum or the 2.4 mm day⁻¹ contour (Ref 70 only). Several studies have examined metrics based on P-E (precipitation minus evaporation) from several sources; an observationally based composite P-E dataset derived

from GPCP and Woods Hole Oceanographic Institute oceanic evaporation data⁷¹ and the output from several reanalysis products.⁵⁸ The global position of the STR, derived from sea level pressure data from three reanalyses and the HadSLP2 dataset,⁸⁴ has also been used to estimate tropical expansion.⁶⁶

Table 6 summarizes these results of the surface-based studies. The multiple studies using GPCP data to examine subtropical precipitation minimum have conflicting results. One study finds that the tropical edge is moving poleward around 0.5–0.7° decade⁻¹ in

TABLE 6 | Summary of Surface-Based Methodologies

Investigators		Data Sources	Metric	Time Period	Expansion (°Latitude Decade ⁻¹)
Hu et al. ⁶⁶	S	GPCP	Subtropical precipitation minimum	1979–2009	SH: 0.52 NH: 0.71
	S	NCEP, ERA40, NCEP2, and HadSLP2	Subtropical ridge location	1979–2009	SH: 0.18 NH: 0.22
Davis and Rosenlof ⁵⁸	S	NCEP, JRA25, CFSR, and MERRA	Subtropical P-E = 0	1979–2009	SH: -0.7 to 2.0 NH: 0.0–0.5
Zhou et al. ⁷⁰	S	GPCP	Subtropical 2.4 mm day ⁻¹ isopleth	1979–2007	SH: 0.4 NH: 0.5
	S	GPCP	Subtropical minimum precipitation	1979–2007	SH: 0.1 NH: 0.0
Allen et al. ⁷¹		GPCP and WHOI evaporation	Subtropical P-E = 0	1979–2009	SH: 0.31 NH: 0.52
		GPCP	Subtropical precipitation minimum	1979–1999	SH: 0.42 NH: 0.31

Positive values equal expansion regardless of hemisphere. An 'S' after the investigators indicates the study examined the seasonality of the expansion. NH, Northern Hemisphere; SH, Southern Hemisphere.

the SH, slightly more in the NH.⁶⁶ Another indicates a slower rate of expansion, with slightly more seen in the SH.⁷¹ The third reports little expansion in either hemisphere using the annual metric, but show considerable expansion in the NH summer; this study reports similar results from estimates using the edge the subtropical dry zone.⁷⁰ The STR metrics suggest a poleward trend of around 0.2° decade⁻¹ in each hemisphere, although there is considerable difference between datasets.⁶⁶ Expansion estimates using P-E as a metric show considerable scatter, particularly in the SH.^{58,71} Little consensus exists among these metrics regarding the strength or timing of the seasonality of the expansion.

Intensity Changes

Changes to the intensity of large-scale tropical circulations—both the HC and the zonal Walker circulation (WC)—have also been reported by several studies. These changes, while not the main focus of the article, are useful in interpreting the expansion results. Table 7 briefly summarizes these findings.

For the HC, the intensity is often estimated using the peak value of Ψ within the cell. Figure 3 shows the time series of this metric for eight reanalyses. In the NH, a significant strengthening of the HC is indicated in five of eight reanalyses. In the SH, the results are mixed, with both strengthening and weakening being identified in different products; only four of eight define a significant trend in either direction. Seasonally the most robust intensification

in these data is observed in NH winter and spring (i.e., DJF and MAM), with the SH and other seasons producing weaker trends, often of a different sign.²¹ Other studies^{85,89} using different approaches generally support these findings, particularly the changes to the strength of the NH winter (DJF) cell. An even stronger trend in the intensity of the DJF winter cell was noted in the ERA40 reanalysis.⁸⁶ A general intensification in the annual average HC intensities in both hemispheres is suggested by a reanalysis ensemble average; two exceptions were noted in the SH.⁸⁰ The interannual variability of the HC using global radiosonde data shows no obvious trend in the data.^{86,87} Satellite data, in particular OLR and reflected shortwave, were used to infer an intensification of the HC.⁶⁶ The interpretation of these results was questioned,⁹⁰ and a subsequent investigation⁹¹ significantly lowered the estimates of radiative imbalance, a result of adjustments for satellite altitude errors and instrument drift. Satellite-derived estimates of water vapor transport indicate an intensification of the HC during DJF, also suggested by reanalysis data.⁸⁸

Studies of the trends in WC are contradictory; decadal variability appears to play a significant role. Weakening trends have been noted in the NCEP reanalysis⁸⁵ and an independent historical sea level pressure dataset.⁹² However, satellite water vapor transport observations suggest that the WC is strengthening since 1979.⁸⁸ On an interannual basis, radiosonde estimates⁸⁷ suggest that the strength of the HC and WC varied in opposition to one another, an observation also supported by satellite data.⁸⁸

TABLE 7 | Summary of the Observed Changes to the Intensity of the Tropical Circulations

Investigator	Subject	Data Source	Comments
Chen et al. ⁶⁷	Broad tropics	Satellite shortwave and longwave fluxes	Intensity shift not quantified; subtle changes to satellite radiances suggestive of intensification of the HC and/or WC
Tanaka et al. ⁸⁵	HC WC	NCEP velocity potential	DJF winter cell is intensifying. No significant trend in JJA WC weakening since (at least) 1979. A strong link the SOI
Mitas and Clement ⁸⁶	DJF winter cell	NCEP/ERA40/NCEP2, isobaric streamfunction Radiosonde [extended Oort and Yienger (1996) series] Ref 87 GCM multimodel ensemble	Trends in peak Ψ : $7.5/21.2/1.2 \times 10^9 \text{ kg s}^{-1} \text{ decade}^{-1}$ for NCEP/ERA40/NCEP2 Trend in peak Ψ : $0.3 \times 10^9 \text{ kg s}^{-1} \text{ decade}^{-1}$ Modeled trends over the 20th century mostly range -10 to $+4 \times 10^9 \text{ kg s}^{-1} \text{ decade}^{-1}$, suggest weakening
Stachnik and Schumacher ⁸⁰	HC	Eight reanalysis ensemble	NH: $4.0 \times 10^9 \text{ kg s}^{-1} \text{ decade}^{-1}$ Ranges from 0.3 to $1.43 \times 10^9 \text{ kg s}^{-1} \text{ decade}^{-1}$ SH: $0.7 \times 10^9 \text{ kg s}^{-1} \text{ decade}^{-1}$ Ranges from -13.9 to $+5.4 \times 10^9 \text{ kg s}^{-1} \text{ decade}^{-1}$
Sohn and Park ⁸⁸	DJF HC DJF WC	NCEP, ERA40, and SSM/I	Intensification of NH winter cell of $\sim 15\text{--}25\%$ since 1979 Intensification of Pacific WC of $\sim 25\%$ since 1979/significant decadal variability, with decrease from mid-20th century to 1979
Nguyen et al. ²¹ (see also Figure 3)	HC	Eight reanalyses	NH: -0.5 to $12.7 \times 10^9 \text{ kg s}^{-1} \text{ decade}^{-1}$ SH: -3.2 to $9.0 \times 10^9 \text{ kg s}^{-1} \text{ decade}^{-1}$

Positive values equal expansion regardless of hemisphere. An 'S' after the investigators indicates the study examined the seasonality of the expansion. HC, Hadley circulation; NH, Northern Hemisphere; SH, Southern Hemisphere; WC, Walker circulation.

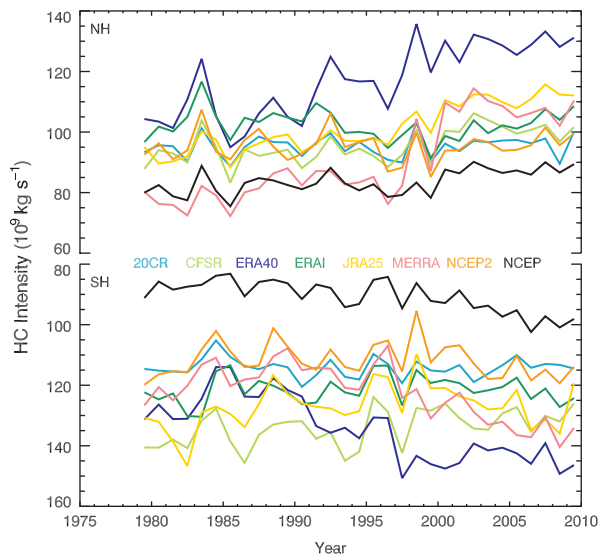


FIGURE 3 | Time series of the peak intensity (vertically-averaged maximum Ψ) of the Hadley cell in the eight reanalyses for the Northern (top) and Southern (bottom) Hemispheres. (Reprinted with permission from Ref 21. Copyright 2013 The American Meteorological Society). Time series from ERA40 (post 2002) and 20CR (post 2008) are partially extrapolated from statistical relations with the other reanalyses Ψ .

SOURCES OF OBSERVATIONAL UNCERTAINTY

As seen in the previous section, considerable uncertainty exists in the observations. While the broad consensus of studies suggests that the tropics are expanding, results from different datasets and methodologies do not necessarily agree. In this section, possible sources of this uncertainty are discussed. In particular, the potential shortcomings of the reanalysis products are addressed, followed by a description of some of the limitations associated with the individual metrics and methodologies.

Reanalysis Considerations

The majority of observational studies of tropical expansion rely on one or more of the eight available reanalysis data products, and this potentially has a wide-ranging effect on the results. These products are a hybrid of numerical weather prediction model output and assimilated data from various observational platforms. They are very useful for climate analysis as they incorporate historical observations in a physically

consistent manner.⁹³ Generally, reanalyses adequately reproduce many mean ‘dynamic’ quantities like wind and temperature, albeit with some systematic error.⁹⁴ Perhaps most importantly, their globally complete spatial and temporal coverage provides information in otherwise data-sparse regions.

However, potential shortcomings remain. A lack of observations may not fully constrain the reanalysis, and allow possibly unrealistic model variability to dominate.⁹⁵ The observational network, particularly the satellite-based components, has evolved considerably over the previous decades, which may introduce inhomogeneities into the reanalyses.^{90,96,97} Comparisons of radiosonde and reanalysis-based estimates of tropical expansion using the THF methodology⁶² indicate that inhomogeneities in reanalysis products may be behind the differences in estimates of tropical expansion.

Further, differences in the physics of the underlying models used within the various reanalyses can result in different representations of the circulation. The strong HC intensification in the ERA40 was demonstrated to be a result of a (unrealistic) tropical mid-tropospheric cooling trend.⁹⁸ The NH winter cells in the NCEP and ERA40 reanalyses show significant differences, driven by the differing cloud amounts and radiation budgets predicted by the two products.⁹⁹ Newer reanalyses are not free from these shortcomings; considerable variability is present in the strength and width of the HC within the different products.^{21,80}

These issues conceivably account for the differences observed in tropical expansion trend estimates across reanalysis products. The differences in performance are readily apparent in Figures 2 and 3, where considerable scatter is noted in the position and strength of the NH and SH Hadley cells. Simpler metrics, like changes to the mean jet stream position, are better-captured by the reanalyses and have less scatter in the estimates. More complex metrics, like tropopause height, Ψ or P-E, are more subject to the vagaries of the reanalysis models and cover a broader range, even within a given metric. The scatter in the estimates is often larger in the SH, where fewer *in situ* observations are available and the reanalyses are more reliant on their internal dynamics and assimilated satellite data.¹⁰⁰ The available evidence, while not conclusive at this time, indicates that these effects are potentially quite significant and cannot be ignored.

Methodological Concerns

In addition to underlying problems with the reanalyses, differences in the expansion rates between

the different methodologies and datasets are, at least to some degree, a manifestation of the differing physics represented by the different metrics.⁵⁸ Further, individual datasets and/or methodologies may introduce their own unique shortcomings. These are described below.

Tropopause-based methods are the most widely used and the most widely critiqued methodology employed to date.^{57,58} Results using this technique are broadly consistent across the range of studies, the initial effort of Seidel and Randel⁵⁵ being the exception. The interpretation of the results from this methodology is relatively straightforward, without relying on too many assumptions, although seasonal variability could confound the results. Identifying the tropopause in the subtropics can be problematic in the reanalyses, but the use of blended tropopause data is promising.⁶¹ The reanalyses do broadly capture the interannual variability of TTD, although the possibility of inhomogeneities and/or other reanalysis issues cannot be discounted.⁶² The use of appropriate relative thresholds^{57,58} is likely important, but needs further work to enhance their robustness. The use of a fixed threshold may account for up to 20% of the total trend due to global background tropopause trends.⁶²

Satellite-based data are subject to many uncertainties. In a study of the shifts of the midlatitude storm track using ISCCP cloud cover data, correction of data problems significantly reduced or even eliminated the trends in the data.¹⁰¹ Similar issues may affect estimates of tropical expansion that use satellite-based metrics and potentially account for the differences in cloudiness-based estimates of tropical expansion, where both corrected⁷¹ and uncorrected⁷⁰ data are used.

Satellite estimates using broadband OLR are a particular concern. The observational data have a strong trend, while modeling studies^{102,103} suggest that net changes to broadband OLR should be relatively small, on the order of 0.5 K or less. One potential factor responsible for the trend—overlooked in tropical expansion studies to date—is a change in the equatorial crossing time (ECT) of the polar-orbiting satellites.¹⁰⁴ This alters the time of day when the satellite views a scene and has been shown to produce significant biases, particularly over land.^{105–107} Figure 4 explores the possible impact on tropical expansion calculations. The left panel shows the uncorrected NOAA OLR data¹⁰⁸; expansionary trends of the 250 W m⁻² contours of 0.82 and -0.32° decade⁻¹ are seen in the NH and SH, respectively. These values are similar to those previously reported using the same dataset and analysis protocol.⁶⁶ Using a dataset that has a statistically based ECT correction¹⁰⁷

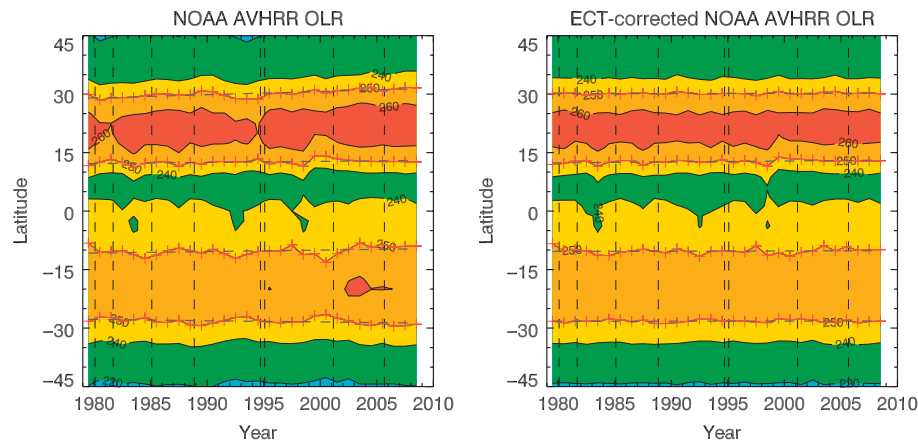


FIGURE 4 | Time-latitude profiles of annually averaged NOAA AVHRR OLR for uncorrected (left) and the equatorial crossing time (ECT)-corrected data (Ref 107) for the period 1979–2008. Vertical dashed lines indicate the changes in the satellite. Contours are every 10 W m^{-2} , with the 250 W m^{-2} contour colored in red. The trend along this contour is also indicated with a dashed line.

applied effectively removes any expansionary trends in the data. While it cannot be absolutely stated that the statistical correction algorithm has not removed a valid long-term climate signal, these results raise questions about the true magnitude of OLR-based estimates of tropical expansion. Clearly, more investigation into this ECT bias and its effects on tropical expansion calculations is warranted.

Further, a physically based model for the interpretation of the OLR in terms of the ‘edge of the tropics’ is required, as opposed to a simple climatological definition. The expected behavior of OLR in response to a changing climate is complex. While changes to overall broadband OLR were small, changes in specific spectral regions could be quite large.¹⁰³ Changes to the surface, tropospheric and stratospheric temperatures all play a role, as does the variability in water vapor, clouds, and aerosol. These effects vary in different portions of the spectrum, with sources often making opposite contributions. Consideration of these effects and the examination of specific spectral regions could lead to more reliable estimates of tropical expansion, and explain any differences in trends between hemispheres.

At first glance, the use of Ψ to identify the HC and the edge of the tropics would appear ideal. It provides an unambiguous, quantitatively defined definition of the tropical edge. In practice, these definitions are sensitive to the differences in the reanalyses, which show significant variations in the strength, width, and position of the HC (Figures 2 and 3). Further, the HC shows a larger degree of seasonality in the trends than other metrics, particularly in the NH. The HC during summer and early autumn is generally weak.²¹ The meridional gradient about the zero-contour is ‘flat’ and as a consequence the identified position of

the tropical edge is sensitive to small perturbations. These seasons are when the tropical expansion trends with this metric are the largest.^{21,58,65} Conceivably, even small errors/uncertainties in the reanalyses could overwhelm the comparatively weak signals at this time of year and result in an artificial trend. Temporal inhomogeneities may also be important here, as significant changes were made to the global observing system in the early 21st century,^{51,54} particularly the addition of new satellite data sources. Conceivably, these could be behind the SH shift noted in Figure 2. Further, the seasonal cycle of width defined from Ψ is different than those defined from the jet streams and $\Delta\theta$ stability parameter, with different amplitude and timing.⁶⁴ More investigation of these effects and their impact on the results is required.

The jet stream methods from reanalysis data^{58,81} and radiosonde data⁷¹ appear to produce reasonably robust results. These results indicate very small (and often not statistically significant) amounts of expansion. These studies tend to be based on the annual or seasonal mean winds; care must be taken to identify the SH STJ during austral summer.⁶⁴ Studies based on maximum winds produce noisier results.⁵⁸ Jet streams objectively identified on daily time scales suggest a more complex behavior of these phenomena,¹⁰⁹ with more than one jet often apparent and a distinct annual cycle in the position and strength of the jet in both hemispheres. How well the mean quantities used in tropical expansion studies represent this complex behavior and what its impact may be are unknown.

The suitability of the other methodologies that have been used to assess the rate of tropical expansion is unclear. In many cases, there are simply not enough studies to support (or refute) their robustness. The source of the disparity between results using the

GPCP subtropical minimum precipitation is unclear, and may reflect the use of different versions of the GPCP dataset (version 2.1 vs 2.2). If this is the case, it suggests a strong sensitivity to the input data. Further, the use of absolute thresholds⁷⁰ with this data needs to be carefully considered; as with the OLR and THF methods, the chosen threshold should be physically linked with the tropical edge, beyond just a climatological coincidence. Other metrics derived from reanalyses (like P-E) are subject to reanalysis uncertainties, particularly in the data-poor SH and should be treated with caution until better understood. The effects of seasonal variability also need consideration with these methods.

MECHANISMS AND FORCINGS BEHIND TROPICAL EXPANSION

In this section, the influences on the position of the tropical edge are examined. Tropical expansion and changes to the HC have been examined in numerous GCMs using paleoclimate, 20th century, and climate change scenarios. From these simulations, physical mechanisms have been proposed. Simulations from simplified GCMs with idealized forcing are instructive. Natural climate forcing factors, as seen through observational studies, can have a significant effect. Modeling also suggests a significant role for anthropogenic influences. Experiments examining the role of individual forcings are described; these climate forcings include greenhouse gases, stratospheric ozone depletion, and aerosols.

Tropical Expansion in CMIP3 and Other Simulations

The GCMs used in the World Climate Research Programme (WCRP) Coupled Model Intercomparison Project phase 3 (CMIP3) multimodel dataset project¹¹⁰ show significant changes to the tropical circulation during the 21st century as a result of increasing greenhouse gas concentrations (generally either the A1B or A2 scenarios), a poleward expansion of the HC of 1°–2° over the 21st century along with a decrease in the intensity of the HC and WC.^{30,67,111,112} Closely associated to this are a shift in the subtropical dry zone and changes to the hydrologic cycle, with wet regions becoming wetter and dry regions drier.¹¹³ Much of this change is hypothesized to be driven by the thermodynamic effects of increasing specific humidity, although dynamic changes also allow the poleward flanks of the HC to dry.¹¹⁴ A recent study¹¹⁵ suggest that the poleward shifts of the MMC are more responsible for subtropical drying than the thermodynamic

effect. On an annual basis, these projected changes are largely symmetric about the equator.⁵⁶

While CMIP3 simulations generally show an expansion of the tropics, uncertainties remain. The strength of the modeled HC across the suite of models varies by a factor of 2.¹¹² Other GCMs outside of the CMIP3 framework are more equivocal in their response. Several studies^{46,116} investigated the HC in simulations of paleo, present day, and future climate simulations, covering a wide ‘parameter space’ in overall temperature, surface characteristics, topography, and solar forcing. Despite the range, changes in the characteristics of the HC were noted between these different eras were generally small. These results highlight the model dependency in the results, owing (at least in part) to the various formulations, parameterizations, and assumptions made within models. One of the studies¹¹⁶ reports that the formulation of the ocean model plays a strong role in determining the final characteristics of the HC. The climate sensitivity of a given model, related to the strength of the feedbacks within the model, can also have an impact on future trends in the circulation.¹¹⁷

As noted in the idealized model of the MMC, a strong interaction exists between the tropics and extratropics. Hence, it seems plausible that variability in the extratropical circulation has an effect on the tropical edge (or vice versa). This is consistent with results³⁶ that identify an interannual relationship between the HC edge and the latitude of the eddy-driven jet in the SH during summer. Similar relationships between the HC extent and the annular modes in both hemispheres have been identified in most reanalysis products, although again not in JJA.²¹ The CMIP3 simulations suggest that tropical expansion is to some degree a consequence of circulation changes in the extratropical portion of the MMC, rather than a driver of those changes. Up to half of the projected change to the subtropical dry zones can be associated with changes to the annular mode.¹¹⁸ Midlatitude dynamics are likely important to the expansion.¹¹⁹ Hadley cell scaling arguments indicate that the extratropical tropopause heights are a better predictor of modeled tropical expansion than tropical tropopause heights.⁵⁶ Overall, the role of tropical–extratropical interactions in tropical expansion remains uncertain, but it appears to be significant.

Proposed Mechanisms of Tropical Expansion

Two potential dynamical mechanisms for tropical expansion have been proposed.²⁹ Both mechanisms require tropical–extratropical interactions and invoke

a poleward shift in the position of extratropical jet stream. The first mechanism involves a reduction in baroclinicity in the subtropics, which dampens eddy activity there and extends the HC further poleward. This reduction is a result of an increase in the (dry) static stability, related to a quasi-moist adiabatic adjustment to increasing specific humidity. A recent study¹²⁰ suggests that changing wind shear characteristics may be more important than static stability changes.

The second mechanism relates to an increase in the phase speed of upper-tropospheric baroclinic waves. The faster moving waves are unable to penetrate as far equatorward, producing a poleward shift in eddy momentum flux convergence and an associated shift in the position of the eddy-driven jet.^{121,122} This may be related to a rising tropopause in the subtropics.¹²³ An examination¹²⁴ of this mechanism in greater detail suggests that a transition in the wave type (equatorward- vs poleward-breaking waves⁴⁰) may also play a role. Changes to the eddy length scale may be a factor,¹²⁵ perhaps in response to an increase in upper-tropospheric baroclinicity in the midlatitudes.¹²⁶

Idealized Simulations

Experiments with simplified GCMs and idealized heating profiles have been used to explore tropical expansion and the shift in the eddy-driven jet stream. Using idealized heating profiles reminiscent of those expected from global warming scenarios, Butler et al.¹²⁷ found that both tropical upper-tropospheric heating and stratospheric cooling resulted in a poleward shift in midlatitude jet and an expansion of the HC. Although qualitatively similar in terms of the jet response, the resulting circulations due to forcings from the two regions were different. Allen et al.¹²⁸ performed a suite of simulations using a range of idealized heating profiles, both stratospheric cooling and tropospheric heating. In their experiments, heating in the deep tropics resulted in little change in jet stream and HC, while midlatitude heating produced a poleward jet shift and expansion of the HC. Tandon et al.¹²⁰ examined the circulation response to a series of tropospheric heating profiles of varying widths. Heating near the equator produced a contraction of the tropics and poleward shift in the jet stream. Subtropical heating produced the opposite responses.

While the model simulations provide a degree of insight into the dynamical mechanisms of tropical expansion, some uncertainty remains. In the idealized runs, the results are sensitive to the choice of initial conditions and the details of the forcing used.

However, the meridional extent of the forcing appears to be particularly important factor in determining the response of the HC in these idealized experiments.

Natural Variability

The position of the tropical edge varies on interannual (and longer) time scales. A primary source of climate variability is ENSO. Both the width and intensity of the HC varies with the phase of ENSO.⁸⁶ During the warm El Niño phase, the HC is narrower and more intense; during La Niña, the opposite is observed. This general tendency is also suggested in GCM simulations,²⁹ which also show an equatorial shift of the STJ during El Niño. The various reanalysis products indicate an intensification⁸⁰ and contraction²¹ of the HC during El Niño compared with Neutral and La Niña phases in reanalyses. Using THF metrics, the expansion and variability were more pronounced in the extratropical portions of the subtropics, less so toward the deep tropics, with changes in width from La Niña to El Niño in the order of 1°–2° latitude.⁶² The Pacific Decadal Oscillation (PDO) has also been hypothesized to impact the width of the tropics. During cool phases of the PDO, the HC is ~1° latitude further poleward compared with its warm phase position. This is primarily observed during the equinox seasons.¹²⁹

Globally significant volcanic eruptions can also have an impact on the tropics. Eruptions can increase stratospheric aerosol, warming the lower stratosphere and lowering tropopause height.¹³⁰ Tropical precipitation can be lowered by ~5%¹³¹ and particularly large eruptions may act as a trigger for El Niño.¹³² A signal of tropical contraction following large eruptions is apparent, particularly in studies using tropopause-based methodologies. The magnitude of this effect is estimated to be ~1° latitude.⁶²

Greenhouse Gases and SST

The relative roles of radiative forcing and SST changes on tropical expansion from 1958 to 2000 have been examined using the THF methodology.⁵⁶ Expansion trends were accurately replicated by the model, with more pronounced trends in the SH. The expansion was attributed to changes in atmospheric radiative forcing; indirect SST changes had little effect. Stratospheric cooling was found to be particularly important in producing the observed trends, although no distinction between the effects of greenhouse gases and stratospheric ozone depletion could be made due to the design of the experiment. Seasonal changes to SST do not appear to account for tropical expansion in CMIP3 simulations, suggesting that

extratropical eddies have induced the expansion.¹¹⁹ Deser and Phillips¹³³ found that the direct effects of atmospheric radiative forcing led to a strengthening and intensification of midlatitude westerly winds in the SH over the latter half of the 20th century. In the NH, SST changes, particularly over the tropics, were responsible for the intensification of the Aleutian low and a weakened WC. While the HC was not specifically examined, an expansionary trend in the SH is implied by the poleward shift of the westerlies. Other studies indicate that as a whole the indirect SST change is the main driver of circulation change from both the preindustrial (1870) to the present period and extending into the future, although factors like ozone depletion may have a significant, but temporary impact on the hemispheric circulation.¹³⁴ Hu et al.⁶⁶ also emphasized that historical SST changes played a significant, but incomplete role in reproducing the observed expansion.

Stratospheric Ozone Depletion

Numerous studies have suggested that stratospheric ozone depletion plays a role in tropical expansion of the SH. For the 20th century, the GCMs in CMIP3 with ozone depletion consistently showed greater tropical expansion through a variety of metrics than those without.¹³⁵ In future scenarios, GCMs with ozone recovery showed on average near zero trends in the tropopause, jet location, HC, and SAM index, in contrast to runs without ozone recovery. These results were only qualitative, as details of the ozone forcing were unavailable. Using seven reanalyses and a multimodel GCM dataset, optimal fingerprinting techniques identified a separable signal of stratospheric ozone depletion in SH tropical expansion during DJF, but not in other seasons.¹³⁶

A multimodel ensemble of 17 climate-chemistry models (CCM) has been used to understand the response of the SH circulation to the effects of explicitly simulated stratospheric ozone depletion.¹³⁷ This study found that ozone depletion in the late-spring led to a poleward shift and intensification of the SH tropospheric jet and an expansion of the HC. These changes to the HC were primarily found during the SH summer. Similar results were obtained using a coupled CCM,¹²⁴ suggesting that the observed changes in the 20th century were better explained by stratospheric ozone changes compared to changing GHG concentrations.

Model simulations using separate ozone and GHG forcings have also suggested that stratospheric ozone depletion was the main driver of 20th century SH climate change. In particular, ozone depletion

resulted in a widening of the HC and an expansion of the SH subtropical dry zones.¹³⁸ In the first half of the 21st century, ozone recovery may approximately cancel the effects of GHG on the MMC, resulting in a reduced rate of expansion.¹³⁹ Other models have suggested that the distinct effects of polar stratospheric ozone depletion could extend well into the SH subtropics, resulting in a precipitation increase at those latitudes.¹⁴⁰

Aerosol

Aerosol forcing of the climate is complex, but quite significant. They can directly affect the radiative flux through scattering (primarily sulfate aerosol) or absorption (e.g., black carbon), contributing to surface cooling and/or atmospheric solar heating.¹⁴¹ Semi-direct and indirect aerosol effects may also impact the climate.¹⁴² The semi-direct effect arises when the heating associated with absorbing aerosols changes relative humidity, impacting the lifetime of clouds. The indirect effects of aerosol involve their interactions with cloud properties, including increasing their albedo and lifetime and alteration of their precipitation characteristics. Modeling studies¹⁴³ suggest that these indirect effects can be approximately of equal magnitude (but oppositely signed) to the forcing by GHG. Further complicating the role of aerosol is their observed regional distribution and relatively short lifetime.¹⁴⁴

Earlier studies have examined aerosol effects on aspects of the tropical circulation, particularly on regional scales. The direct effects of increasing black carbon may intensify the Asian summer monsoon, while increases of only scattering aerosol weakens the circulation.¹⁴⁵ The indirect aerosol effect may drive a southward shift in the ITCZ, potentially associated with past Sahelian drought.¹⁴⁶ While aerosol loadings are regional in scope, they can have circulation impacts at remote regions around the globe.^{147,148}

Aerosol impacts on the broader MMC have also been reported. The direct effects of black carbon included a northward displacement of the ITCZ and a strengthened (weakened) HC in the Northern (Southern) Hemisphere.¹⁴⁸ Anthropogenic aerosols (largely absorbing) weaken the HC and shift the peak streamfunction northward. Natural aerosols (mostly reflecting) had the opposite effects. Opposing shifts in the STJ were also noted, with anthropogenic aerosols shifting the jet stream poleward in both hemispheres.¹⁴⁹ The observed shift in the NH tropics has been attributed to midlatitude heating by black carbon aerosol and tropospheric ozone. The modeled response was notably less than that observed in reality.⁷¹ Model simulations that included smoke

aerosol from landscape fires showed a widening and weakening of the HC.¹⁵⁰

The response of the tropical circulation to both direct and indirect aerosol effects has been modeled.¹⁵¹ Radiative cooling from aerosol is most prominent in the NH, creating an interhemispheric radiative imbalance. The atmosphere attempts to moderate this asymmetry by altering the zonal-mean circulation in the tropics, resulting in a weaker (stronger) HC in the Northern (Southern) Hemisphere. The asymmetrical portions of the circulation (i.e., the WC) strengthen in both hemispheres. In the zonal-mean, the subtropics (defined here as 20°–30° latitude) of both hemisphere become wetter. However, the authors conclude that the atmospheric responses may be overestimated because of a lack of an interactive ocean model in these simulations.

SYNTHESIS

A variety of methodologies have been used to examine tropical expansion. Most studies begin at the start of the satellite era (1979) and extend into the first decade of the 21st century. Figure 5 summarizes the rates of expansion estimated by these studies, stratified into the methodological categories discussed earlier. The numerous studies indicate a robust poleward expansion of the tropical edges of both hemispheres over the last ~30 years. Almost all studies suggest that the rate of expansion in each hemisphere has been less than 1° decade⁻¹, with many suggesting rates around half of that value. Many of these widening trends may not be statistically significant at the 95% level.⁵⁸ Tropopause-based studies generally suggest a greater widening in the SH; satellite-based studies indicate the opposite. Studies using Ψ suggest a greater seasonality and an (highly uncertain) intensification of the HC. As a whole, jet stream metrics suggest a generally smaller rate of expansion. Taken together, a total expansion of 1°–3° latitude in each hemisphere is implied since 1979.

The seasonality of the changes, if any, is unclear. Some metrics, notably the Ψ -based findings, show strong seasonality with the largest changes in each hemisphere's respective summer and autumn.^{21,65} Jet stream metrics based on the position of the peak zonal-mean 850 hPa zonal wind show notable seasonal differences in the SH.⁵⁸ Seasonal variability is suggested in other metrics,^{58,70} but many of these differences are not statistically significant.⁵⁸ As noted earlier, some of the metrics, particularly during the warm season, may not produce robust results.

Modeling studies suggest that multiple climate forcings can result in an expansion of the

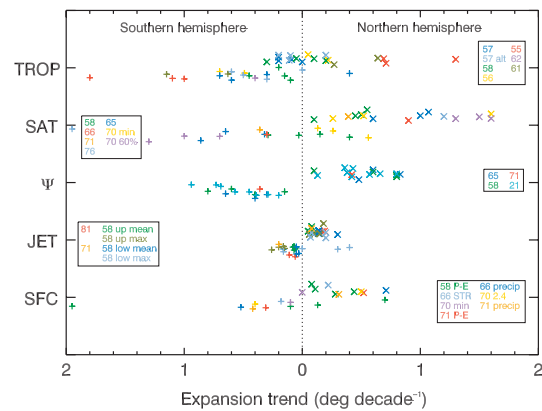


FIGURE 5 | Summary of result of observational tropical expansion studies, broken down by categories. Pluses (+) represent SH values, crosses (x) NH values of tropical expansion trend. Symbols in the corresponding hemisphere indicates expansion, symbols in the 'opposite' hemisphere indicate contraction. Within a particular methodology, the vertical position of each symbol is randomized to improve clarity of individual symbols; no other meaning is implied. Colors of symbols refer to source and/or methodology, with legends for each category in boxes to side of plot, where numbers represent the cited reference.

tropics, including increasing GHG concentrations and associated changes to the SST, stratospheric ozone depletion (particularly in the SH) and the effects of aerosols, both direct and indirect. Each of these forcings results in subtly different impacts on the tropical edge, as summarized in Table 8. A comparison of these projections with the relevant climatological variables can provide a qualitative assessment of the relative importance of these factors.

Tropical expansion is noted in both the NH and the SH, suggesting some degree of symmetry in the response. This suggests that the observed increase in specific humidity (water vapor),^{152–154} associated with the increase in GHG and global temperature, is playing a role in tropical expansion. However, the observations of HC intensity, while highly uncertain, suggest no trend or a slight intensification, which is inconsistent with this response. Some studies^{111,151} suggest that this thermodynamic effect may impact the zonal WC more than the HC. Most studies, but not all, report that the WC has weakened in recent decades, although internal climate variability may account for a significant fraction of the observed weakening.¹⁵⁵

During the 20th century, zonal-mean precipitation has increased in the SH tropics and subtropics, while decreasing in the NH.¹⁵⁶ Coupled climate models indicate that these changes are a result of anthropogenic radiative forcing, with GHG and sulfate aerosol forcing specifically noted. Kang et al.¹⁴⁰ also report a similar tendency in the subtropical

TABLE 8 | Summary of Tropical Expansion Projections Following Different Forcings

Forcing	Citations	Projected Effects
A2, A1B (many contain ozone, but generally O3 recovery when evaluated)	Lu et al., ⁵⁶ Seager et al. ¹¹⁴	Expansion rate: 0.1–0.2° decade ⁻¹ Symmetric about equator Weakening and expansion of HC Reduction of precipitation in subtropics Enhancement of rain in ITCZ/monsoon Poleward shift in jet
Stratospheric ozone depletion	Son et al., ¹³⁵ Son et al., ¹³⁷ Polvani et al., ¹³⁹ Kang et al., ¹⁴⁰ Staten et al., ¹³⁴ Min and Son ¹³⁶	Greater impact in SH spring and summer SH subtropical precipitation increase HC widening and poleward shift in SH
Direct aerosol (sulfate)	Wang, ¹⁴⁸ Allen et al. ⁷¹	Strengthened HC Equatorward shift in jet stream
Direct aerosol (black carbon)	Wang, ¹⁴⁸ Allen et al. ⁷¹	Weakening of HC Northward shift in ITCZ Poleward shift of jet stream
Indirect aerosol	Rostayn and Lohmann, ¹⁴⁶ Rotstayn et al., ¹⁴⁷ Ming and Ramaswamy ¹⁵¹	Asymmetric response—intensification of SH HC, weakening in NH Precipitation increase in subtropics Southward shift in ITCZ
Sea surface temperature	Hu et al., 2011, ⁶⁵ Deser and Phillips, ¹³³ Staten et al. ¹³⁴	Poleward shift in jet stream

precipitation in the SH, but attribute the increase to stratospheric ozone depletion. As noted in earlier, a considerable amount of modeling evidence exists for a significant role of stratospheric ozone depletion in producing SH tropical expansion, although these changes are largely confined to the SH spring and summer seasons. Some degree of SH asymmetry in expansion rates is observed in tropopause-based metrics, but not in others (Figure 5).

Aerosols, particularly from volcanoes, clearly play a role in tropical expansion on interannual time scales, but longer term effects are unlikely. The asymmetric expansion (in some results) and precipitation response is reminiscent of the indirect aerosol effect,¹⁴³ a forcing that has not been included in many climate simulations to date, including the CMIP3 archive. However, the evidence for this factor is unclear; little change has been observed in either a proxy for the global ITCZ²¹ or in the satellite-detected eastern Pacific ITCZ¹⁵⁷ and the apparent HC intensification has occurred in both hemispheres, more in the NH. The role of direct aerosol effects is also incomplete; while Allen et al.⁷¹ explicitly attribute NH expansion to black carbon aerosol and tropospheric ozone, the projected response is considerably less than the observed increase.

The dynamical mechanisms behind tropical expansion are unclear, but many hypotheses proposed to date^{29,122,124} indicate that the extratropics and

baroclinic eddies play a significant role. One manifestation of this is a poleward shift in the storm track, closely associated with the position of the eddy-driven jet stream. Yin¹⁵⁸ notes this as a response to climate change in simulations of the 21st century. Bender et al.¹⁰¹ identified such a shift in recent decades, albeit with some reservations due to data issues. Overall, a shift in the storm track results in less precipitation over subtropical regions, with this mechanism possibly more important than the thermodynamic effect.¹¹⁵ Other modeling studies have indicated a close linkage of the jet position and the HC.^{135,137} Relationships between the HC edge (identified using the Ψ methodology) and the jet stream position have been identified for some seasons, particularly in the SH.^{21,36} A poleward shift in the jet stream is also closely related to poleward shift in the annular mode. Up to half of the projected change to the subtropical dry zones may be associated with changes to the annular mode.¹¹⁸

To summarize, no clear consensus exists regarding the primary forcing mechanism behind tropical expansion. Any singular forcing generally results in an under-prediction of the observed amount of tropical expansion.⁷⁹ This may reflect a shortcoming of the modeling approaches used to date; for example, the models simply are not correct or sensitive enough to reproduce the observed changes. Certainly, given the varied response of the

different models in play, this suggestion cannot be dismissed out-of-hand. However, it may be that tropical expansion simply does not have a single cause. Rather, it may arise from a variety of causes that have acted in concert to produce the observed response, with different factors acting in the NH and SH. Other factors not thoroughly considered to date by modeling may also play a role. The atmosphere is complex, and an attempt to attribute the whole change to a single forcing may not be appropriate.

OUTSTANDING ISSUES

As summarized in this review, considerable efforts have been made within the climate community to understand the causes and effects of tropical expansion. From this research a coherent picture is emerging, but many gaps remain in our knowledge. These are briefly summarized below.

A key issue is the determination of the true rate of tropical expansion. A broad consensus from current studies suggests the value is below $1^\circ \text{decade}^{-1}$, but which hemisphere is expanding at a faster rate (if either) remains unclear. Also unclear is the seasonality of the expansion, with significant differences identified between the various methodologies. Developing a clearer picture requires improving our understanding and interpretation of current methodologies used to estimate tropical expansion, as well as the formulation of new ones. Clarifying the linkages between different metrics is crucial. For example, do THF methods tell us the same thing as Ψ methods? Addressing data quality issues through homogenized datasets and/or reanalysis products is paramount.

One particular shortcoming in our understanding is the role of tropical–extratropical interaction in the MMC. To what degree does tropical expansion arise from changes in the extratropical circulation? Several studies discussed herein suggest that

the changes to the extratropics may be the source of the tropical expansion. Traditionally in the atmospheric sciences, the tropics, and extratropics have been treated as separate entities. To overcome this, a new conceptual framework of understanding for the hemispheric (and global) MMC is required. The idealized model shown earlier provides a qualitative description of such a framework, a useful starting point.

Another significant issue is the understanding of the climate factors responsible for tropical expansion. This includes not only identifying the most significant climate forcings, but also the dynamical mechanisms by which they act. This requires the ongoing efforts of model development and evaluation, as well as observational studies to propose new hypotheses and verify the results. A sharper focus on the seasonality and/or longitudinal variability of the expansion could improve the understanding of the hypothesized forcings. The current understanding of many potential forcings (e.g., the role of aerosol in the climate) remains uncertain. It is helpful to understand the tropical expansion observed to date, which can then lead to a better interpretation of projected climate futures.

Finally, a better understanding of the impacts of tropical expansion on the climate and society is required. Much of the research to date has focused on the global or zonal-mean responses to expansion, e.g., the subtropical dry zone will expand. Some studies have identified this as a factor in recently observed SH rainfall declines.¹⁵⁹ However, questions remain about what this means at a given location in the subtropics. For instance, GCM simulations often indicate a significant regional variability in the response. The reality of the MMC is more complicated than that presented in a simple zonal-mean picture. For purposes of planning and climate adaptation, a better understanding of regional responses to tropical expansion is required.

ACKNOWLEDGMENTS

This research was funded as part of the South Eastern Australia Climate initiative Phase 2 (SEACI 2). Interpolated OLR data were provided by the NOAA/OAR/ESRL PSD, Boulder, CO, USA, from their Web site <http://www.esrl.noaa.gov/psd/>. The ECT-corrected version of the same dataset was provided by Matt Sapiano. Tim Cowan, Pandora Hope, and two anonymous reviewers provided helpful comments on the manuscript.

REFERENCES

1. CSIRO (Commonwealth Scientific and Industrial Research Organisation). *Climate and Water Availability in South-eastern Australia: A Synthesis of Findings from Phase 2 of the South Eastern Australian Climate Initiative (SEACI)*. Australia: CSIRO; 2012, 41 pp.

2. Indian Ocean Climate Initiative. *Western Australia's Weather and Climate: A Synthesis of Indian Ocean Climate Initiative Stage 3 Research*. Australia: CSIRO and BoM; 2012.
3. Hoerling M, Eischeid J, Perlwitz J, Quan X, Zhang T, Pegion P. On the increased frequency of Mediterranean drought. *J Clim* 2012, 25:2146–2161. doi: 10.1175/JCLI-D-11-00296.1.
4. Sousa PM, Trigo RM, Aizpurua P, Nieto R, Gimeno L, Garcia-Herrera R. Trends and extremes of drought indices throughout the 20th century in the Mediterranean. *Nat Hazards Earth Syst Sci* 2011, 11:33–51.
5. Cayan DR, Das T, Pierce DW, Barnett TP, Tyree M, Gershunov A. Future dryness in the southwest US and the hydrology of the early 21st century drought. *Proc Natl Acad Sci USA* 2010, 107:21271–21276. doi: 10.1073/pnas.0912391107.
6. Morales MS, Christie DA, Villalba R, Argollo J, Pacajes J, Silva JS, Alvarez CA, Llanabure JC, Soliz Gamboa CC. Precipitation changes in the South American Altiplano since 1300 AD reconstructed by tree-rings. *Clim Past* 2012, 8:653–666. doi: 10.5194/cp-8-653-2012.
7. Ye J-S. Trend and variability of China's summer precipitation during 1955–2008. *Int J Climatol* 2013. doi: 10.1002/joc.3705.
8. Dai A. Drought under global warming: a review. *WIREs Clim Change* 2011, 2:45–65. doi: 10.1002/wcc.81.
9. Dai A. Increasing drought under global warming in observations and models. *Nat Clim Change* 2012, 3: 52–58. doi: 10.1038/nclimate1633.
10. Mueller B, Seneviratne S. Hot days induced by precipitation deficits at the global scale. *Proc Natl Acad Sci USA* 2012, 109:12398–12403. doi: 10.1073/pnas.1204330109.
11. Mishra AK, Singh VP. A review of drought concepts. *J Hydrol* 2010, 391:202–216. doi: 10.1016/j.hydrol.2010.07.012.
12. Kenyon J, Hegerl GC. Influence of modes of climate variability on global precipitation extremes. *J Clim* 2010, 23:6248–6262. doi: 10.1175/2010JCLI3617.1.
13. Seidel DJ, Fu Q, Randel WJ, Reichler TJ. Widening of the tropical belt in a changing climate. *Nat Geosci* 2008, 1:21–24. doi: 10.1038/ngeo.2007.38.
14. Reichler T. Changes in the atmospheric circulation as an indicator of climate change. In: Letcher TM, ed. *Climate Change: Observed Impacts on Planet Earth*. Amsterdam: Elsevier; 2009, 145–164.
15. Townsend RD, Johnson DR. A diagnostic study of isentropic zonally averaged mass circulation during the First GARP Global Experiment. *J Atmos Sci* 1985, 42:1565–1579. doi: 10.1175/1520-0469(1985)042<1565:ADSOTI>2.0.CO;2.
16. Schneider T. The general circulation of the atmosphere. *Annu Rev Earth Planet Sci* 2006, 34:655–688. doi: 10.1146/annurev.earth.34.031405.125144.
17. Pauluis OA, Czaja A, Korty R. The global atmospheric circulation on moist isentropes. *Science* 2008, 321:1075–1078. doi: 10.1126/science.1159649.
18. Pauluis OA, Czaja A, Korty R. The global atmospheric circulation in moist isentropic coordinates. *J Clim* 2010, 23:3077–3093. doi: 10.1175/2009JCLI12789.1.
19. Fierro AO, Simpson J, LeMone MA, Straka JM, Smull BF. On how hot towers fuel the Hadley cell: an observational and modelling study of line-organized convection in the equatorial trough from TOGA-COARE. *J Atmos Sci* 2009, 66:2730–2746. doi: 10.1175/2009JAS3017.1.
20. Webster PJ. The elementary Hadley circulation. In: Diaz HF, Bradley RS, eds. *The Hadley Circulation: Past, Present and Future*. Dordrecht: Kluwer Academic Publishers; 2005, 9–60.
21. Nguyen H, Evans A, Lucas C, Smith I, Timbal B. The Hadley circulation in reanalyses: climatology, variability and expansion. *J Clim* 2013, 26:3357–3376. doi: 10.1175/JCLI-D-12-00224.
22. Schneider EK, Lindzen RS. Axially symmetric steady-state models of the basic state for instability and climate studies. Part I: linearized calculations. *J Atmos Sci* 1977, 34:263–279. doi: 10.1175/1520-0469(1977)034<0263:ASSMO>2.0.CO;2.
23. Held IM, Hou AY. Nonlinear axially symmetric circulations in a nearly inviscid atmosphere. *J Atmos Sci* 1980, 37:515–533. doi: 10.1175/1520-0469(1980)037<0515:NASCIA>2.0.CO;2.
24. Frierson DMW, Lu J, Chen G. Width of Hadley cell in simple and comprehensive general circulation models. *Geophys Res Lett* 2007, 34:L18804. doi: 10.1029/2007GL031115.
25. Rind D, Rossow WB. The effects of physical processes on the Hadley circulation. *J Atmos Sci* 1984, 41:479–507. doi: 10.1175/1520-0469(1984)041<0479:TEOPPO>2.0.CO;2.
26. Walker C, Schneider T. Eddy influences on Hadley circulations: Simulations with an idealized GCM. *J Atmos Sci* 2006, 63:3333–3350. doi: 10.1175/JAS3821.1.
27. Palmén E, Newton CW. *Atmospheric Circulation Systems*. New York: Academic Press; 1969, 603.
28. Held IM. The General Circulation of the Atmosphere. Presented at the 2000 Woods Hole Oceanographic Institute Geophysical Fluid Dynamics Program. Woods Hole, MA: Woods Hole Oceanogr. Inst.; 2000. Available at: <http://www.whoi.edu/fileserver.do?id=21464&pt=10&p=17332>. (Accessed September 9 2013)
29. Lu J, Chen G, Frierson DMW. Response of the zonal mean atmospheric circulation to El Niño versus

- global warming. *J Clim* 2008, 21:5835–5851. doi: 10.1175/2008JCLI2200.1.
30. Lu J, Vecchi GA, Reichler T. Expansion of the Hadley cell under global warming. *Geophys Res Lett* 2007, 34:L06805. doi: 10.1029/2006GL028443.
31. Kang SM, Lu J. Expansion of the Hadley Cell under global warming: winter versus summer. *J Clim* 2012, 25:8387–8393. doi: 10.1175/JCLI-D-12-00323.1.
32. Limpasuvan V, Hartmann DL. Wave-maintained annular modes of climate variability. *J Clim* 2000, 13:4414–4429. doi: 10.1175/1520-0442(2000)013<4414:WMAMOC>2.0.CO;2.
33. Karoly DJ, McIntosh PC, Berrisford P, McDougall TJ, Hirst AC. Similarities of the Deacon cell in the Southern Ocean and the Ferrel cells in the atmosphere. *Q J R Meteorol Soc* 1997, 123:519–526. doi: 10.1002/qj.49712353813.
34. Galewsky J, Sobel A, Held I. Diagnosis of subtropical humidity dynamics using tracers of last saturation. *J Atmos Sci* 2005, 62:3353–3367. doi: 10.1175/JAS3533.1.
35. Bordoni S, Schneider T. Monsoons as eddy-mediated regime circulations of the tropical overturning circulation. *Nat Geosci* 2008, 1:515–519. doi: 10.1038/ngeo248.
36. Kang SM, Polvani LM. The interannual relationship between the latitude on the eddy-driven jet and the edge of the Hadley Cell. *J Clim* 2011, 24:563–568. doi: 10.1175/2010JCLI4077.1.
37. Ding Q, Steig EJ, Battisti DS, Wallace JM. Influence of the tropics on the Southern Annular Mode. *J Clim* 2012, 25:6330–6348. doi: 10.1175/JCLI-D-11-00523.1.
38. Moore RW, Martius O, Spengler T. The modulation of the subtropical and extratropical atmosphere in the Pacific basin in response to the Madden-Julian Oscillation. *Mon Weather Rev* 2010, 138:2761–2779. doi: 10.1175/2010MWR3194.1.
39. Solomon S. Stratospheric ozone depletion: a review of concepts and history. *Rev Geophys* 1999, 37:275–316. doi: 10.1029/1999RG900008.
40. Wittman MAH, Charlton AJ, Polvani LM. The effect of lower stratospheric shear on baroclinic instability. *J Atmos Sci* 2007, 64:479–496. doi: 10.1175/JAS3828.1.
41. Solomon S, Rosenlof KH, Portman RW, Daniel JS, Davis SM, Sanford TJ, Plattner G-K. Contributions of stratospheric water vapour to decadal changes in the rate of global warming. *Science* 2010, 327:1219–1222. doi: 10.1126/science.1182488.
42. Maycock AC, Joshi MM, Shine KP, Scaife AA. The circulation response to idealized changes in stratospheric water vapour. *J Clim* 2012, 26:545–561. doi: 10.1175/JCLI-D-12-00155.1.
43. Baldwin MP, Dunkerton TJ. Stratospheric harbingers of anomalous weather regimes. *Science* 2001, 294:581–584. doi: 10.1126/science.1063315.
44. Cook KH. Role of continents in driving the Hadley cells. *J Atmos Sci* 2003, 60:957–976. doi: 10.1175/1520-0469(2003)060<0957:ROCIDT>2.0.CO;2.
45. Becker E, Schmitz G. Interaction between extratropical stationary waves and the zonal mean circulation. *J Atmos Sci* 2001, 58:462–480. doi: 10.1175/1520-0469(2001)058<0462:IBESWA>2.0.CO;2.
46. Rind D, Perlwitz J. The response of the Hadley circulation to climate changes, past and future. In: Diaz HF, Bradley RS, eds. *The Hadley Circulation: Past, Present and Future*. Dordrecht: Kluwer Academic Publishers; 2004, 399–436.
47. Kalnay E, Kanamitsu M, Kistler R, Collins W, Deaven D, Gandin L, Iredell M, Saha S, White G, Woollen J, et al. The NMC/NCAR 40-year reanalysis project. *Bull Am Meteorol Soc* 1996, 77:437–471. doi: 10.1175/1520-0477(1996)077<0437:TNYRP>2.0.CO;2.
48. Uppala SM, Kallberg PW, Simmons AJ, Andrae U, Da Costa BV, Fiorino M, Gibson JK, Haseler J, Hernandez A, Kelly GA, et al. The ERA-40 reanalysis. *Q J R Meteorol Soc* 2005, 131:2961–3012. doi: 10.1256/qj.04.176.
49. Kanamitsu M, Ebisuzakai W, Woollen J, Yang S-K, Hnilo JJ, Fiorino M, Potter GL. NCEP-DOE AMIP-II reanalysis (R-2). *Bull Am Meteorol Soc* 2002, 83:1631–1643. doi: 10.1175/BAMS-83-11-1631.
50. Onogi K, Tsutsui J, Koide H, Sakamoto M, Kobayashi S, Hatsushika H, Matsumoto T, Yamazaki N, Kamahori H, Takahashi K, et al. The JRA-25 reanalysis. *J Meteorol Soc Jpn* 2007, 85:369–432.
51. Dee DP, Uppala SM, Simmons AJ, Berrisford P, Poli P, Kobayashi S, Andrae U, Balmaseda MA, Balsamo G, Bauer P, et al. The ERA-Interim reanalysis: configuration and performance of the data assimilation system. *Q J R Meteorol Soc* 2011, 137:553–597. doi: 10.1002/qj.828.
52. Saha S, Moorthi S, Pan H-L, Wu X, Wang J, Nadiga S, Tripp P, Kistler R, Woollen J, Behringer D, et al. The NCEP climate forecast system reanalysis. *Bull Am Meteorol Soc* 2010, 91:1015–1057. doi: 10.1175/2010BAMS3001.1.
53. Compo GP, Whitaker JS, Sardeshmukh PD, Matsui N, Allan RJ, Yin X, Gleason BE, Vose RS, Rutledge G, Bessemoulin P, et al. The twentieth century reanalysis project. *Q J R Meteorol Soc* 2011, 137:1–28. doi: 10.1002/qj.776.
54. Rienecker MM, Suarez MJ, Gelaro R, Todling R, Bacmeister J, Liu E, Bosilovich MG, Schubert SD, Takacs L, Kim G-K, et al. MERRA: NASA's modern-era retrospective analysis for research and applications. *J Clim* 2011, 24:3624–3648. doi: 10.1175/JCLI-D-11-00015.1.

55. Seidel DJ, Randel WJ. Variability and trends in the global tropopause estimated from radiosonde data. *J Geophys Res* 2007, 111:D21101. doi: 10.1029/2006JD007363.
56. Lu J, Deser C, Reichler T. Cause of the widening of the tropical belt since 1958. *Geophys Res Lett* 2009, 36:L03803. doi: 10.1029/2008GL036076.
57. Birner T. Recent widening of the tropical belt from global tropopause statistics: sensitivities. *J Geophys Res* 2010, 115:D23109. doi: 10.1029/2010JD014664.
58. Davis SM, Rosenlof KH. A multi-diagnostic inter-comparison of tropical width time series using reanalyses and satellite observations. *J Clim* 2012, 25:1061–1078. doi: 10.1175/JCLI-D-11-00127.1.
59. Seidel DJ, Randel WJ. Variability and trends in the global tropopause estimated from radiosonde data. *J Geophys Res* 2006, 111:D21101. doi: 10.1029/2006JD007363.
60. Schmidt T, Wickert J, Beyerle G, Heise S. Global tropopause heights estimated from GPS radio occultation. *Geophys Res Lett* 2008, 35:L23802. doi: 10.1029/2008GL035820.
61. Wilcox LJ, Hoskins BJ, Shine KP. A global blended tropopause based on ERA data. Part II: trends and tropical broadening. *Q J R Meteorol Soc* 2012, 138: 576–584. doi: 10.1002/qj.910.
62. Lucas C, Nguyen H, Timbal B. An observational analysis of Southern Hemisphere tropical expansion. *J Geophys Res* 2012, 117:D17112. doi: 10.1029/2011JD017033.
63. Reichler T, Dameris M, Sausen R. Determining the tropopause height from gridded data. *Geophys Res Lett* 2003, 30:2042–2046. doi: 10.1029/2003GL018240.
64. Davis NA, Birner T. Seasonal to multi-decadal variability of the width of the tropical belt. *J Geophys Res* 2013, 118:7773–7787. doi: 10.1002/jgrd.50610.
65. Hu Y, Fu Q. Observed poleward expansion of the Hadley circulation since 1979. *Atmos Chem Phys* 2007, 7:5229–5236. doi: 10.5194/acp-7-5229-2007.
66. Hu Y, Zhou C, Liu J. Observational evidence for the poleward expansion of the Hadley circulation. *Adv Atmos Sci* 2011, 28:33–44. doi: 10.1007/s00376-010-0032-1.
67. Chen J, Carlson BE, Del Genio AD. Evidence for strengthening of the tropical general circulation in the 1990s. *Science* 2002, 295:838–841. doi: 10.1126/science.1065835.
68. Wielecki BA, Wong T, Allen RP, Slingo A, Kiehl JT, Soden BJ, Gordon CT, Miller AJ, Yang S-K, Randall DA, et al. Evidence for large decadal variability in the tropical mean radiative energy budget. *Science* 2002, 295:841–844. doi: 10.1126/science.1065837.
69. Hatzidimitriou D, Vardavas I, Pavlakis KG, Hatzianastassiou N, Matsoukas C, Drakakis E. On the decadal increase in the tropical mean outgoing longwave radiation for the period 1984–2000. *Atmos Chem Phys* 2004, 2004:1419–1425. doi: 10.5194/acp-4-1419-2004.
70. Zhou YP, Xu K-M, Sud YC, Betts AK. Recent trends of the tropical hydrological cycle inferred from Global Precipitation Climatology Project and International Satellite Cloud Climatology Project data. *J Geophys Res* 2011, 116:D09101. doi: 10.1029/2010JD015197.
71. Allen RJ, Sherwood SC, Norris JR, Zender CS. Recent Northern Hemisphere tropical expansion primarily driven by black carbon and tropospheric ozone. *Nature* 2012, 485:350–354. doi: 10.1038/nature11097.
72. Rossow WB, Schiffer RA. ISCCP cloud data products. *Bull Am Meteorol Soc* 1991, 72:2–20. doi: 10.1175/1520-0477(1991)072<0002:ICDP>2.0.CO;2.
73. Jacobowitz H, Stowe LL, Ohring G, Heidinger A, Knapp K, Nalli NR. The Advanced Very High Resolution Radiometer Pathfinder Atmosphere (PATMOS) climate data set: a resource for climate research. *Bull Am Meteorol Soc* 2003, 84:785–793. doi: 10.1175/BAMS-84-6-785.
74. Hudson RD, Andrade MF, Follette MB, Frolov AD. The total ozone field separated into meteorological regimes—Part II: Northern hemisphere mid-latitude total ozone trends. *Atmos Chem Phys* 2006, 6:5183–5191. doi: 10.5194/acp-6-5183-2006.
75. Hudson RD, Frolov AD, Andrade MF, Follette MB. 2003: The total ozone field separated into meteorological regimes. Part I: defining the regions. *J Atmos Sci* 2003, 60:1669–1677. doi: 10.1175/1520-0469(2003)060<1669:TTOFSI>2.0.CO;2.
76. Hudson RD. Measurements of the movement of the jet streams at mid-latitudes, in the Northern and Southern Hemispheres, 1979 to 2010. *Atmos Chem Phys* 2012, 12:7797–7808. doi: 10.5194/acp-12-7797-2012.
77. Fu Q, Johanson CM, Wallace JM, Reichler T. Enhanced mid-latitude tropospheric warming in satellite measurements. *Science* 2006, 312:1179. doi: 10.1126/science.1125566.
78. Fu Q, Lin P. Poleward shift of subtropical jets inferred from satellite-observed lower-stratospheric temperatures. *J Clim* 2011, 24:5597–5603. doi: 10.1175/JCLI-D-11-00027.1.
79. Johanson CM, Fu Q. Hadley cell widening: model simulations versus observations. *J Clim* 2009, 22:2713–2725. doi: 10.1175/2008JCLI2620.1.
80. Stachnik JP, Schumacher C. A comparison of the Hadley circulation in modern reanalyses. *J Geophys Res* 2011, 116:D22102. doi: 10.1029/2011JD016677.
81. Archer CL, Caldeira K. Historical trends in the jet streams. *Geophys Res Lett* 2008, 35:L08803. doi: 10.1029/2008GL033614.

82. Adler RF, Huffman GJ, Chang A, Ferraro R, Xie P-P, Janowiak J, Rudolf B, Schneider U, Curtis S, Bolvin D, et al. The version 2 Global Precipitation Climatology Project (GPCP) monthly precipitation analysis (1979–Present). *J Hydrometeorol* 2003, 4:1147–1167. doi: 10.1175/1525-7541(2003)004<1147:TVGPCP>2.0.CO;2.
83. Huffman GJ, Adler RF, Bolvin DF, Gu G. Improving the global precipitation record: GPCP version 2.1. *Geophys Res Lett* 2009, 36:L17808. doi: 10.1029/2009GL040000.
84. Allan RJ, Ansell TJ. A new globally complete monthly historical mean sea level pressure data set (HadSLP2):1850–2004. *J Clim* 2006, 19:5816–5842. doi: 10.1175/JCLI3937.1.
85. Tanaka HL, Ishizaki N, Kitoh A. Trend and interannual variability of Walker, monsoon and Hadley circulations defined by velocity potential in the upper troposphere. *Tellus* 2004, 56A:250–269. doi: 10.1111/j.1600-0870.2004.00049.x.
86. Mitas CM, Clement A. Has the Hadley cell been strengthening in recent decades? *Geophys Res Lett* 2005, 32:L03809. doi: 10.1029/2004GL021765.
87. Oort AH, Yienger JJ. Observed interannual variability in the Hadley circulation and its connection to ENSO. *J Clim* 1996, 9:2751–2767. doi: 10.1175/1520-0442(1996)009<2751:OIVITH>2.0.CO;2.
88. Sohn BJ, Park S-C. Strengthened tropical circulations in past three decades inferred from water vapour transport. *J Geophys Res* 2010, 115:D15112. doi: 10.1029/2009JD013713.
89. Quan X-W, Diaz HF, Hoerling MP. Change in the tropical Hadley cell since 1950. In: Diaz HF, Bradley RS, eds. *The Hadley Circulation: Past, Present and Future*. Dordrecht: Kluwer Academic Publishers; 2004, 85–120.
90. Trenberth KE. Changes in tropical clouds and radiation. *Science* 2005, 2002:296. doi: 10.1126/science.296.5576.2095a.
91. Wong T, Wielicki BA, Lee RB, Smith GL, Bush KA, Willis JK. Reexamination of the observed decadal variability of the Earth radiation budget using altitude-corrected ERBE/ERBS nonscanner WFOV data. *J Clim* 2006, 19:4028–4040. doi: 10.1175/JCLI3838.1.
92. Vecchi GA, Soden BJ, Wittenberg AT, Held IM, Leetmaa A, Harrison MJ. Weakening of tropical Pacific atmospheric circulation due to anthropogenic forcing. *Nature* 2006, 441:73–76. doi: 10.1038/nature04744.
93. Thorne PW, Vose RS. Reanalyses suitable for characterizing long-term trends. *Bull Am Meteorol Soc* 2010, 91:353–361. doi: 10.1175/2009BAMS2858.1.
94. Reichler T, Kim J. Uncertainties in the climate mean state of global observations, reanalyses and the GFDL climate model. *J Geophys Res* 2008, 113:D05106. doi: 10.1029/2007JD009278.
95. Sterl A. On the (in)homogeneity of reanalysis products. *J Clim* 2004, 17:3866–3873. doi: 10.1175/1520-0442(2004)017<3866:OTIORP>2.0.CO;2.
96. Trenberth KE, Stepaniak DP, Hurrell JW, Fiorno M. Quality of reanalysis in the tropics. *J Clim* 2001, 14:1499–1510. doi: 10.1175/1520-0442(2001)014<1499:QORITT>2.0.CO;2.
97. Bengtsson L, Hagemann S, Hodges KI. Can climate trends be calculated from reanalysis data? *J Geophys Res* 2004, 109:D11111. doi: 10.1029/2004JD004536.
98. Mitas CM, Clement A. Recent behaviour of Hadley Cell and tropical thermodynamics in climate models and re-analyses. *Geophys Res Lett* 2006, 33:L01810. doi: 10.1029/2005GL024406.
99. Song H, Zhang M. Changes of the boreal winter Hadley Circulation in the NCEP-NCAR and ECMWF Reanalyses: a comparative study. *J Clim* 2007, 20:5191–5200. doi: 10.1175/JCLI4260.1.
100. Bengtsson L, Hodges KI, Hagemann S. Sensitivity of the ERA40 reanalysis to the observing systems: determination of the global atmospheric circulation from reduced observations. *Tellus* 2004, 56A:456–471. doi: 10.1111/j.1600-0870.2004.00079.x.
101. Bender FA-M, Ramanathan V, Tselioudis G. Changes in extratropical storm track cloudiness 1983–2008: observational support for a poleward shift. *Clim Dyn* 2012, 38:2037–2053. doi: 10.1007/s00382-011-1065-6.
102. Huang Y, Ramaswamy V, Soden B. An investigation of the sensitivity of the clear-sky outgoing longwave radiation to atmospheric temperature and water vapour. *J Geophys Res* 2007, 112:D05104. doi: 10.1029/2005JD006906.
103. Huang Y, Ramaswamy V. Evolution and trend of the outgoing longwave radiation spectrum. *J Clim* 2009, 22:4637–4651. doi: 10.1175/2009JCLI2874.1.
104. Ignatov A, Laszlo I, Harrod ED, Kidwell KB, Goodrum GP. Equator crossing times for NOAA, ERS and EOS sun-synchronous satellites. *Int J Remote Sensing* 2004, 25:5255–5266. doi: 10.1080/01431160410001712981.
105. Waliser DE, Zhou W. Removing satellite equatorial crossing time biases from the OLR and HRC datasets. *J Clim* 1997, 10:2125–2146. doi: 10.1175/1520-0442(1997)010<2125:RSECTB>2.0.CO;2.
106. Lee H-T, Gruber A, Ellingson RG, Laszlo I. Development of the HIRS outgoing longwave radiation climate dataset. *J Atmos Oceanic Tech* 2007, 24:2029–2047. doi: 10.1175/2007JTECHA989.1.
107. Sapiano MRP, Janowiak JE, Smith TM, Arkin PA, Xie P, Lee H. Correction for temporal discontinuities in the OPI. *J Atmos Oceanic Tech* 2010, 27:457–469. doi: 10.1175/2009JTECHA1366.1.
108. Liebmann B, Smith CA. Description of a complete (Interpolated) outgoing longwave radiation dataset. *Bull Am Meteorol Soc* 1996, 77:1275–1277.

109. Koch P, Wernli H, Davies HUW. An event-based jet-stream climatology and typology. *Int J Climatol* 2006, 26:283–301. doi: 10.1002/joc.1255.
110. Meehl GA, Covey C, Delworth T, Latif M, McAvaney B, Mitchell JFB, Stouffer RJ, Taylor KE. The WCRP CMIP3 multi-model dataset: a new era in climate change research. *Bull Am Meteorol Soc* 2007, 88:1383–1394. doi: 10.1175/BAMS-88-9-1383.
111. Vecchi GA, Soden BJ. Global warming and the weakening of the tropical circulation. *J Clim* 2007, 20:4316–4340. doi: 10.1175/JCLI4258.1.
112. Gastineau G, Le Truet H, Li L. Hadley circulation changes under global warming conditions indicated by coupled climate models. *Tellus* 2008, 60A:863–884. doi: 10.1111/j.1600-0870.2008.00344.x.
113. Held I, Soden BJ. Robust responses of the hydrological cycle to global warming. *J Clim* 2006, 19:5686–5699. doi: 10.1175/JCLI3990.1.
114. Seager R, Niak N, Vecchi GA. Thermodynamic and dynamic mechanisms for large-scale changes in the hydrological cycle in response to global warming. *J Clim* 2010, 23:4651–4668. doi: 10.1175/2010JCLI13655.1.
115. Scheff J, Frierson D. Twenty-first century multi-model subtropical precipitation declines are mostly midlatitude shifts. *J Clim* 2012, 25:4330–4347. doi: 10.1175/JCLI-D-11-00393.1.
116. Otto-Bliesner BL, Clement A. The sensitivity of the Hadley circulation to past and future forcings in two climate models. In: Diaz HF, Bradley RS, eds. *The Hadley Circulation: Past, Present and Future*. Dordrecht: Kluwer Academic Publishers; 2005, 437–464.
117. Arblaster JM, Meehl GA, Karoly DJ. Future climate change in the Southern Hemisphere: competing effects of ozone and greenhouse gases. *Geophys Res Lett* 2011, 38:L02701. doi: /10.1029/2010GL045384.
118. Previdi M, Liepert BG. Annular modes and Hadley cell expansion under global warming. *Geophys Res Lett* 2007, 34:L22701. doi: 10.1029/2007GL031243.
119. Sobel AH, Camargo SJ. Projected future seasonal changes in tropical summer climate. *J Clim* 2011, 24:473–487. doi: 10.1175/2010JCLI3748.1.
120. Tandon NF, Gerber EP, Sobel AH, Polvani LM. Understanding Hadley cell expansion vs. contraction: insights from simplified models and implications for recent observations. *J Clim* 2013, 26:4304–4321. doi: 10.1175/JCLI-D-12-00598.1.
121. Chen G, Held IM. Phase speed spectra and the recent poleward shift of Southern Hemisphere surface westerlies. *Geophys Res Lett* 2007, 34:L21805. doi: 10.1029/2007GL031200.
122. Chen G, Lu J, Frierson DMW. Phase speed spectra and the latitude of surface westerlies: Interannual variability and the global warming trend. *J Clim* 2008, 21:5942–5959. doi: 10.1175/2008JCLI2306.1.
123. Lorenz DJ, DeWeaver ET. Tropopause height and zonal wind response to global warming in the IPCC scenario integrations. *J Geophys Res* 2007, 112:D10119. doi: 10.1029/2006JD008087.
124. McLandress C, Shepherd T, Scinocca J, Plummer D, Sigmond M, Jonsson A, Reader C. Separating the dynamical effects of climate change and ozone depletion: Part 2. Southern hemisphere troposphere. *J Clim* 2011, 24:1850–1868. doi: 10.1175/2010JCLI3958.1.
125. Kidston J, Dean SM, Renwick JA, Vallis GK. A robust increase in the eddy length scale in the simulation of future climates. *Geophys Res Lett* 2010, 37:L03806. doi: 10.1029/2009GL041615.
126. Rivière G. A dynamical interpretation of the poleward shift of the jet stream in global warming scenarios. *J Atmos Sci* 2011, 2011:1253–1272. doi: 10.1175/2011JAS3641.1.
127. Butler AH, Thompson DWJ, Heikes R. The steady-state atmospheric circulation response, to climate change-like thermal forcings in a simple general circulation model. *J Clim* 2010, 23:3474–3496. doi: 10.1175/2010JCLI3228.1.
128. Allen RJ, Sherwood SC, Norris JR, Zender CS. The equilibrium response to idealized thermal forcings in a comprehensive GCM: implications for recent tropical expansion. *Atmos Chem Phys* 2012, 12:4795–4816. doi: 10.5194/acp-12-4795-2012.
129. Grassi B, Redaelli G, Canziani PO, Visconti G. Effects of the PDO Phase on the tropical belt width. *J Clim* 2012, 25:3282–3290. doi: 10.1175/JCLI-D-11-00244.1.
130. Santer BD, Wehner MF, Wigley TML, Sausen R, Meehl GA, Taylor KE, Ammann C, Arblaster J, Washington WM, Boyle JS, et al. Contributions of anthropogenic and natural forcing to recent tropopause height changes. *Science* 2003, 301:479–483. doi: 10.1126/science.1084123.
131. Gu G, Adler RF, Huffman GJ, Curtis S. Tropical rainfall variability on interannual-to-interdecadal and longer time scales derived from the GPCP monthly product. *J Clim* 2007, 20:4033–4046. doi: 10.1175/JCLI14227.1.
132. Emile-Geay J, Seager R, Cane MA, Cook ER, Haug GH. Volcanoes and ENSO over the past millennium. *J Clim* 2008, 21:3134–3148. doi: 10.1175/2007JCLI1884.1.
133. Deser C, Phillips AS. Atmospheric circulation trends, 1950–2000: the relative role of sea surface temperature forcing and direct atmospheric radiative forcing. *J Clim* 2009, 22:396–413. doi: 10.1175/2008JCLI2453.1.
134. Staten PW, Rutz JJ, Reichler T, Lu J. Breaking down the tropospheric circulation response by forcing. *Clim Dyn* 2012, 39:2361–2375. doi: 10.1007/s00382-011-1267-y.

135. Son S-W, Tandon NF, Polvani LM, Waugh DW. Ozone hole and southern hemisphere climate change. *Geophys Res Lett* 2009, 36:L15705. doi: 10.1029/2009GL038671.
136. Min S-K, Son S-W. Multimodel attribution of the Southern Hemisphere Hadley cell widening: Major role of ozone depletion. *J Geophys Res* 2013, 118:3007–3015. doi: 10.1002/jgrd.50232.
137. Son S-W, Gerber EP, Polvani LM, Gillett NP, Seo K-H, Eyring V, Shepherd TG, Waugh D, Akiyoshi A, Austin J, et al. Impact of stratospheric ozone on Southern Hemisphere circulation change: a multimodel assessment. *J Geophys Res* 2010, 115:D00M07. doi: 10.1029/2010JD014271.
138. Polvani LM, Waugh DW, Correa GJP, Son S-W. Stratospheric ozone depletion: the main driver of twentieth-century atmospheric circulation changes in the Southern Hemisphere. *J Clim* 2011, 24:795–812. doi: 10.1175/2010JCLI3772.1.
139. Polvani LM, Previdi M, Deser C. Large cancellation, due to ozone recovery, of future Southern Hemisphere atmospheric circulation trends. *Geophys Res Lett* 2011, 38:L04707. doi: 10.1029/2011GL046712.
140. Kang SM, Polvani LM, Fyfe JC, Sigmond M. Impact of polar ozone depletion on subtropical precipitation. *Science* 2011, 332:951–954. doi: 10.1126/science.1202131.
141. Ramanathan V, Crutzen PJ, Kiehl JT, Rosenfeld D. Aerosols, climate and the hydrological cycle. *Science* 2001, 294:2119–2124. doi: 10.1126/science.1064034.
142. Lohmann U, Feichter J. Global indirect aerosol effects: a review. *Atmos Chem Phys* 2005, 5:715–737. doi: 10.5194/acp-5-715-2005.
143. Ming Y, Ramaswamy V. Nonlinear climate and hydrological responses to aerosol effects. *J Clim* 2009, 22:1329–1339. doi: 10.1175/2008JCLI2362.1.
144. Chung CE, Ramanathan V, Kim D, Podgorny IA. Global anthropogenic aerosol direct forcing derived from satellite and ground-based observations. *J Geophys Res* 2005, 110:D24207. doi: 10.1029/2005JD006536.
145. Randles CA, Ramaswamy V. Absorbing aerosols over Asia: a geophysical fluid dynamics laboratory general circulation models sensitivity study of model response to aerosol optical depth and aerosol absorption. *J Geophys Res* 2008, 113:D21203. doi: 10.1029/2008jd010140.
146. Rotstain LD, Lohmann U. Tropical rainfall trends and the indirect aerosol effect. *J Clim* 2002, 15:2103–2116. doi: 10.1175/1520-0442(2002)015<2103:TRTATI>2.0.CO;2.
147. Rotstain LD, Cai W, Dix MR, Farquhar GD, Feng Y, Ginoux P, Herzog M, Ito A, Penner JE, Roderick ML, et al. Have Australian rainfall and cloudiness increased due to the remote effects of Asian anthropogenic aerosols? *J Geophys Res* 2007, 112:D09202. doi: 10.1029/2006JD007712.
148. Wang C. Impact of direct radiative forcing of black carbon aerosols on tropical convective precipitation. *Geophys Res Lett* 2007, 34:L05709. doi: 10.1029/2006GL028416.
149. Allen RJ, Sherwood RC. The impact of natural versus anthropogenic aerosols on atmospheric circulation in the Community Atmospheric Model. *Clim Dyn* 2011, 36:1959–1978. doi: 10.1007/s00382-010-0898-8.
150. Tosca MG, Randerson JT, Zender CS. Global impact of smoke aerosols from landscape fires on climate and the Hadley circulation. *Atmos Chem Phys* 2013, 13:5227–5241. doi: 10.5194/acp-13-5227-2013.
151. Ming Y, Ramaswamy V. A model investigation of aerosol-induced changes in tropical circulation. *J Clim* 2011, 24:5125–5133. doi: 10.1175/2011JCLI4108.1.
152. Willett KM, Gillett NP, Jones PD, Thorne PW. Attribution of observed surface humidity changes to human influence. *Nature* 2007, 449:710–713. doi: 10.1038/nature06207.
153. Dai A. Recent climatology, variability and trends in global surface humidity. *J Clim* 2006, 19:3589–3606. doi: 10.1175/JCLI3816.1.
154. Lucas, C. A high-quality humidity database for Australia. CAWCR Technical Report No. 024; 2010, 162 pp. Available at: <http://www.cawcr.gov.au/publications/technicalreports.php>. (Accessed September 02, 2013)
155. Power SB, Kociuba G. What caused the observed twentieth-century weakening of the Walker Circulation? *J Clim* 2011, 24:6501–6514. doi: 10.1175/2011JCLI4101.1.
156. Zhang X, Zwiers FW, Hegerl GC, Lambert FH, Gillett NP, Solomon S, Stott PA, Nozawa T. Detection of human influence on twentieth century precipitation trends. *Nature* 2007, 448:461–465. doi: 10.1038/nature06025.
157. Bain CL, De Paz J, Kramer J, Magnusdottir G, Smyth P, Stern H, Wang C-C. Detecting the ITCZ in instantaneous satellite data using spatiotemporal statistical modelling: ITCZ climatology in the east Pacific. *J Clim* 2011, 24:216–230. doi: 10.1175/2010JCLI13716.1.
158. Yin JH. A consistent poleward shift of the storm tracks in simulations of 21st century climate change. *Geophys Res Lett* 2005, 32:L18701. doi: 10.1029/2005GL023684.
159. Cai W, Cowan T, Thatcher M. Rainfall reductions over Southern Hemisphere semi-arid regions: the role of subtropical dry zone expansion. *Sci Rep* 2012, 2:702. doi: 10.1038/srep00702.